Neoplasms and novel gammaherpesviruses in critically endangered captive European minks (Mustela lutreola)

Neoplasms and novel gammaherpesviruses in critically endangered captive European minks (Mustela lutreola)

Journal:	*Transboundary and Emerging Diseases*
Manuscript ID	TBED-OA-270-20.R1
Manuscript Type:	Original Article
Date Submitted by the Author:	23-Jun-2020
Complete List of Authors:	Nicolas, Olga; The University of Edinburgh Royal Dick School of Veterinary Studies Esperon, F.; CISA-INIA, Juan-Sallés, Carles; Noah's Path Ewbank, Ana; Universidade de Sao Paulo, Deparment of Pathology das Neves, Carlos; Norwegian Veterinary Institute Marco Valle, Alberto; Universitat Autònoma de Barcelona Facultat de Veterinària, Departament de Sanitat i d'Anatomia Animals Neves, Elena; CISA-INIA, Group of Epidemiology and Environmental Health Anderson, Neil; The University of Edinburgh Royal Dick School of Veterinary Studies Sacristán, Carlos; Universidade de Sao Paulo, Departamento de Patologia, Faculdade de Medicina Veterinaria e Zootecnia
Subject Area:	herpesvirus, lymphoma, mustelid, Conservation, Wildlife, Diagnostics, Virus

Neoplasms and novel gammaherpesviruses in critically endangered captive European minks (*Mustela lutreola*)

Running title: Neoplasms and gammaherpesviruses in European minks

Olga Nicolas de Francisco[1], Fernando Esperón[2], Carles Juan-Sallés[3], Ana Carolina Ewbank[4], Carlos G. das Neves[5], Alberto Marco[6], Elena Neves[2], Neil Anderson[1] and Carlos Sacristán[2,4,*]

[1]The Royal (Dick) School of Veterinary Studies and the Roslin Institute, University of Edinburgh, Roslin, EH25 9RG, UK.

[2]Group of Epidemiology and Environmental Health, Animal Health Research Center (INIA-CISA).Valdeolmos, Madrid, 28130, Spain.

[3]Noah's Path, Elche, Alicante, 03203, Spain.

[4]Laboratory of Wildlife Comparative Pathology, Department of Pathology, School of Veterinary Medicine and Animal Sciences, University of São Paulo, São Paulo, SP, 05508-270, Brazil.

[5]Norwegian Veterinary Institute. Oslo, PO Box 750 Sentrum, Norway.

[6]Departament de Sanitat i d'Anatomia Animals, Facultat de Veterinària, Universitat Autònoma de Barcelona (UAB), Bellaterra-Barcelona, 08193, Spain.

*Corresponding author: Carlos Sacristán, Laboratory of Wildlife Comparative Pathology, Department of Pathology, School of Veterinary Medicine and Animal Sciences, University of São Paulo, São Paulo, SP, Av. Prof. Dr. Orlando Marques de Paiva, 87, 05508-270, Brazil; Tel: +55 11 981 121 073; Email: carlosvet.sac@gmail.com

SUMMARY

The European mink (*Mustela lutreola*) is a riparian mustelid, considered one of the most endangered carnivores in the world. Alpha, beta, and gammaherpesviruses described in mustelids have been occasionally associated with different pathological processes. However, there is no information about the herpesviruses species infecting European minks. In this study, 141 samples of swabs (oral, conjunctival, anal), feces and tissues from 23 animals were analyzed for herpesvirus (HV) using a pan-HV PCR assay. Two different, potentially novel, gammaherpesvirus species were identified in 12 samples from four animals (17.3%), and tentatively named Mustelid gammaherpesvirus-2 (MUGHV-2) and MuGHV-3. Gross examination was performed on~~in~~ dead minks (n=11), while histopathology was performed ~~in~~ using available samples from HV-positive individuals (n=2), identifying several neoplasms, including B-cell lymphoma (identified by immunohistochemistry) with intralesional syncytia and intranuclear inclusion bodies characteristic of HV (n=1), pulmonary adenocarcinoma (n=1), and biliary (n=1) and preputial (n=1) cystadenoma, as well as other lesions (e.g., axonal vacuolar degeneration [n=2] and neuritis [n=1]). Viral particles, consistent with HVs, were observed by electron microscopy in the mink with neural lymphoma and inclusion bodies. This is the first description of neoplasms and concurrent gammaherpesvirus infection in European minks. The pathological, ultrastructural and PCR findings (MuGHV-2) in the European mink with lymphoma strongly suggest a potential role for this novel gammaherpesvirus in its pathogenesis, as it has been reported in other HV-infected species with lymphoma. The occurrence of neural lymphoma with intralesional syncytia and herpesviral inclusions is, however, unique among mammals. Further research is warranted to elucidate the potential oncogenic properties of gammaherpesviruses in European mink, and their epidemiology in the wild population.

Keywords: biliary cystadenoma, herpesvirus, lymphoma, lung adenocarcinoma, mustelid, preputial cystadenoma.

INTRODUCTION

The European mink (*Mustela lutreola*) is a critically endangered riparian mustelid with populations in eastern (Ukraine, Russia, Estonia and Romania) and western (south-western France and northern Spain) Europe (Maran et al., 2016). The main factors causing its decline are interspecies competition with the non-native American mink (*Neovison vison*), habitat loss and degradation (pollution), over-hunting, and infectious diseases (e.g., Aleutian mink disease and canine distemper) (Lodé et al., 2001; Maran et al., 2016; Mañas et al., 2016a). Without the implementation of more effective conservation measures, the European mink will very likely soon become extinct in Spain (Ferrer, 2014).

To date, the exposure to, and infection by, several viruses have been studied in wild European minks: *Aleutian mink disease virus* (Mañas et al., 2001; Fournier-Chambrillon et al., 2004; Guzmán et al., 2008; Mañas et al., 2016b), *Canine morbillivirus* (syn. canine distemper virus) (Mañas et al., 2001; Guzmán et al., 2008; Philippa et al., 2008), canine parainfluenza virus (syn. parainfluenza virus type 5 or *Mammalian rubulavirus 5*), canine adenovirus (syn. *Canine mastadenovirus A*), and viruses belonging to the families *Astroviridae*, *Picobirnaviridae*, and *Parvoviridae* subfamily *Parvovirinae* (Bodewes et al., 2014). Nevertheless, in spite of the numerous members of the family *Herpesviridae* of veterinary and public health significance (Huff & Barry, 2003; Widén et al., 2012), to the authors' knowledge, there is no information about herpesviruses (HVs) in European minks. The HVs infecting vertebrates (family *Herpesviridae*) are further subdivided into three subfamilies: *Alphaherpesvirinae*, *Betaherpesvirinae* and *Gammaherpesvirinae* (ICTV, 2017). In other mustelid species, for example the sea otter (*Enhydra lutris*), HV-like intranuclear inclusion bodies along with HV-compatible virions, and exposure to herpesvirus have been described (Reimer & Lipscomb, 1998; Goldstein et al., 2011). Alpha-, beta- and gammaherpesviruses (α-HVs, β-HVs, γ-HVs) were identified in American martens (*Martes Americana*) with no mention to associated disease (Dalton et al., 2017). Only γ-HV infection has been reported in other mustelids: in oral ulcerations and plaques, and nasal secretions of sea otters (Tseng et al., 2012); in ulcerative skin lesions of a captive fisher (*Martes pennanti*) (Gagnon et al., 2011); and in free-living European badgers (*Meles meles*) (Banks et al., 2002; Dandár et al., 2010, Sin et al., 2014), in which a γ-HV has not yet been associated with lesions or clinical disease (King et al., 2004). Finally, the susceptibility to α-HV *Suid alphaherpesvirus 1*, the etiological agent of Aujesky'

disease/pseudorabies (Gorham et al., 1998; Quiroga et al., 1997; Liu et al., 2017; Wang et al., 2018) and the replication of α-HV *Canine herpesvirus-1* in fetal lung cells (Reading & Field, 1999) have been reported in American mink.

The goals of this study were to: (1) survey if HVs are present in a European mink captive population; and (2) describe the clinical and pathological findings with a particular focus on morphological evidence of an association with herpesviral infection.

MATERIALS AND METHODS

Study population and samples

This study was performed on the captive European mink population of the Pont de Suert Captive Breeding Center (Pont de Suert, Lleida, northeastern Spain) which is part of the Spanish Breeding Program. Ethical approval for this study was granted by the R(D)SVS Veterinary Ethical Review Committee (VERC, process number 57.17) and the Government of Catalonia (Wildlife and Plant Service within the Department of Sustainability and Territory).

The European mink samples were obtained from the live animal collection of the Pont de Suert captive collection in September 2017 (identified as LM = live mink) and from the dead mink stored at that center until October 2017 (identified as PM = postmortem mink). All these mink were either originated from Spanish captive breeding centers or captured in the wild, also in Spain. Individual sex, last weight, date and place of birth (when available), origin, and arrival date to Pont de Suert, and date of death or euthanasia are summarized in Appendix 1. All European minks in Pont de Suert tested negative for *Aleutian mink disease virus* and *Canine morbillivirus* antibodies upon their admission to the captive breeding program.

In September 2017, all live adult European mink in the breeding center were anesthetized for routine health check with a combination of intramuscular ketamine (5 mg/kg, Imalgene 100 mg/mL, Merial Laboratorios SA, Barcelona, Spain) and medetomidine (0.1 mg/kg, Domtor, Ecuphar Veterinaria SLU, Barcelona, Spain). Intramuscular atipamezole (0.1 mg/kg, Antisedan, Zoetis SLU, Madrid, Spain) was used to reverse the effects of medetomidine a minimum of 20 minutes after anesthesia had been induced. All animals were individually placed back into their cages after sampling and full recovery. During anesthesia, all mink received a full clinical examination by an experienced veterinarian, which included body condition assessment, skin and hair inspection for ectoparasites, abdominal palpation and general examination of the mucosae,

oral cavity, ears, anal-genital region and feet, and cardiac and pulmonary auscultation. Approximately 2 ml of blood were withdrawn by venipuncture from the cranial vena cava using 21-gauge 3.8-cm needles for hematology, biochemistry (data not shown), and molecular analysis (0.5 mL in a sterile eppendorf). Aside from 0.5 mL of whole blood, sterile oropharyngeal, conjunctival and anal swabs were also collected for molecular analysis, and preserved frozen at -20 ºC. Fresh fecal samples were taken from the cages using a sterile tube and refrigerated for direct observation and egg flotation techniques with zinc sulphate (33%) for endoparasite detection (data not shown) or frozen (-20 ºC) to perform viral DNA detection.

Molecular diagnostics

A total of 141 frozen tissue samples from 23 European minks were analyzed by PCR for HV detection. Anal and conjunctival swabs, blood, and feces from live mink (n=12) and representative tissue samples from carcasses (n=10) (Appendix 2) were submitted for PCR analysis. One additional animal was sampled while alive and after its death (codes LM-9 and PM-9), thus included in both categories (live animal and carcasses, Appendix 2). After a lysis step with lysis buffer (Cell Signaling Technology, MA, USA), DNA extraction was performed by pressure filtration (QuickGene DNA tissue kit S, FujiFilm Life Science, Tokyo, Japan). Initially, a mediastinal neoplastic tissue mass from PM-1 (index case) was analyzed by a nested pan-PCR that amplified a fragment of approximately 215-315 bp of the HV DNA polymerase gene (VanDevanter et al., 1996). A second PCR was performed to amplify a 500 bp fragment of the HV glycoprotein B gene for gammaherpesviruses (Ehlers et al., 2008). In order to explore the presence of the novel HV sequence obtained from the neoplastic tissue, a comprehensive HV screening in tissues and samples from the captive breeding center (both live and dead animals) was performed using the PCR described by Ehlers et al. (2008). All glycoprotein B gene-positive samples were also tested for herpesviral DNA polymerase gene (VanDevanter et al., 1996).

The PCR products of DNA polymerase and glycoprotein B were ~~read~~ visualized in 1.5% agarose gel stained with Red Safe® (Ecogen, Spain), and the amplicons of expected size were directly sequenced with sequencing primers TGVseq and IYGseq (DNA polymerase), and 2760s and 2761as (glycoprotein B), respectively described by VanDevanter et al. (1996) and Ehlers et al. (2008). The obtained sequences were compared to those previously published in GenBank using a Blast search, and nucleotide (nt) and deduced amino acid (aa) p-distances were calculated with

MEGA Software 7.0 after editing out the primers (Kumar et al., 2016). After ClustalW alignment of glycoprotein B gene nucleotide sequences by MEGA software 7.0 (Kumar et al., 2016), nt and aa maximum likelihood phylogenetic trees were generated with 1000 bootstrap replicates, including the newly identified HV sequences and 39 other α-, β-, and γ-HVs sequences. *Ictalurid herpesvirus 1* was selected as an outgroup. Sequence information for members of the *Herpesviridae* family was obtained from GenBank.

Gross and microscopic examination

Complete postmortem gross examination was performed in eleven European mink (identified with codes PM-1 through PM-11). Eight of them (PM-2 – PM-8, and PM-10) were prominently autolyzed. Microscopic evaluation was performed on HV-PCR-positive animals with adequate tissue preservation (PM-1 and PM-9), using 10% formalin-fixed tissues embedded in paraffin, sectioned at 5 µm-thick, and stained with hematoxylin and eosin.

Immunohistochemistry

Immunohistochemical analyses were performed in 4 µm-thick paraffin wax-embedded tissue samples of PM-1 using antibodies against CD20 and CD3. Briefly, slides were transferred to a PT-Link Automatic System of DAKO for deparaffinization, rehydration and epitope retrieval. For this last step, slides were treated with acid buffer at pH 6 for 20 min. at 98ºC, and then transferred to distilled water. Endogenous peroxidase was then inhibited with Peroxidase-Blocking Solution (from Dako, Ref.: S2023). Immunostaining was performed on a Dako Autostainer Plus, using procedures, buffers and solutions provided by the fabricant. Briefly, as first antibody, a poly~~i~~clonal Rabbit Anti- Human CD3 antibody (DAKO. Ref: A0452) and a poly~~i~~clonal Rabbit Anti- Human CD20 antibody (CULTEK. Ref: PA5-32313) were both incubated for 40 min. at room temperature, diluted 1:100 (CD3) and 1:200 (CD20) in EnVision™ FLEX buffer. After washing, the Rabbit/Mouse EnVision Detection System (Dako Ref.: K5007) was incubated at room temperature for 40 min, at the dilution recommended by the ~~fabricant~~supplier. After washing, slides were incubated for 5 min. in DAB-Chromogen-hydrogen peroxide (Dako K3468), to reveal binding. After washing, slides were counterstained in Mayer's haematoxylin for 10 seconds, washed in running tap water, and then automatically dehydrated, cleared and mounted.

Electron microscopy

Transmission electron microscopy (TEM) was performed in a paraffin-embedded sample of a perineural mass found in PM-1. The tissue sample was deparaffinized with histoclear, dehydrated with 100% ethanol, infiltrated with LRWhite, sectioned into 60 nm sections and contrasted with uranylacetate. Micrographs were obtained using a FEI Morgagni 268 transmission electron microscope and images were recorded by a side-mounted Olympus Veleta CCD charge-coupled device camera.

RESULTS

Molecular study

Herpesvirus DNA was detected in four (PM-1, PM-4, PM-8, and LM/PM-9) out of the 23 evaluated European minks. Positive HV amplification was observed in 8.5% (12/141) of the analyzed samples, including 11 from postmortem tissue samples and one from an antemortem oral swab (LM/PM-9) (Appendix 2).

Two different glycoprotein B gene sequences were detected in the four HV-positive European mink; one sequence was amplified from PM-1 (mediastinal mass) and PM-8 (lung), and a different one from PM-4 (liver, kidney, brain), and LM/PM-9 (an antemortem oral swab, brain, spinal cord, peripheral nerve [sciatic nerve and brachial plexus], spleen, and bone marrow). The nt and aa identities between both novel glycoprotein B sequences were 79.9% and 86.0%, respectively. The first sequence, found in PM-1 and PM-8, was more similar to the sequence detected in a European badger (MuGHV-1, GenBank Accession number: ABF15169) with, correspondingly, nt and aa identities of 87.2% and 97.8%. The second sequence, found in PM-4 and LM/PM-9, was more related to *Lynx rufus* gammaherpesvirus-2 (ABF15169), with nt identity of 78.4%, and had the highest aa identity (86.0%) with a γ-HV identified in a harp seal (KP136799). A phylogenetic tree based on glycoprotein B amino acid deduced sequences correctly classified the two obtained novel sequences within the cluster of terrestrial mammal γ-HVs, genus *Percavirus*, with bootstrap values above 70% (Figure 1).

A DNA polymerase sequence was amplified in one of the four HV-positive animals (PM-1), while no amplification for that gene was observed in the remaining glycoprotein B gene-positive cases. The highest nt (86.5%) and aa (92.2%) identities of this sequence were to the fisher gammaherpesvirus (HM579931) obtained in another mustelid species, the fisher. The DNA polymerase sequence of PM-1 was submitted to GenBank database under accession number

MN082678, while the glycoprotein B sequences obtained from PM-1 and PM-9 were submitted under accession numbers MN082679 and MN082680, respectively. Since there was a previous report using the terms "Mustelid gammaherpesvirus" (Mustelid gammaherpesvirus-1 or MuGHV-1, Kent et al. [2018]), we have tentatively named the two novel sequences as MuGHV-2 (PM-1 and PM-8) and MuGHV-3 (PM-4 and LM/PM-9). A summary of the γ-HVs detected in mustelids is provided in Table 1.

Retrieval of information prior to death or euthanasia of HV-positive mink

Prior to death, PM-1 presented with corneal opacity in the left eye, protrusion of right eye, severe incoordination, and rear limb weakness, leading to traumatic lesions and inability to eat. PM-4 presented with poor fur quality and compromised vision. PM-8 was uncoordinated and eventually recumbent, which lead to a skin ulcer on its right hip. LM/PM-9 presented with corneal opacity in the left eye and bilateral impaired vision, mild incoordination, rear limbs weakness, and hyporexia that progressed to anorexia. In order to prevent suffering and based on a full clinical examination and complementary examinations (hematology and biochemistry, data not shown), two old animals (over nine years of age; PM-1 and LM/PM-9) were humanely euthanized due to the rapid worsening of clinical signs.

Gross and microscopic findings

The gross and histopathologic findings of the HV-positive mink (PM-1, PM-4, PM-8 and LM/PM-9) are summarized in Appendix 3. The main gross and microscopic findings and suspected cause of death in PM-1 and LM/PM-9 are described below.

PM-1 was a 647-grams male with moderate to severe atrophy of adipose tissue. Protrusion of the right eye due to the presence of a grayish to greenish retrobulbar mass involving the eyelid and peri-ocular skin (Figure 2). The left eye had corneal opacity. Nerves in the left brachial plexus and left elbow joint nerves were surrounded by whitish masses up to 1 cm in greatest dimension (Figure 2). A similar but smaller lesion surrounded the right sciatic nerve distal to the coxofemoral joint. A 5.5x2.8x2.2-cm whitish mass was also found in the caudal mediastinum (Figure 2). The left adrenal gland was partly effaced by a grayish mass 1 cm in diameter (Figure 2).

Microscopically, all masses consisted of a malignant neoplastic proliferation of round cells

characterized by a round, oval, or more rarely irregular, indented or reniform nucleus with 1-2 nucleoli and diverse chromatin patterns, and a low amount of eosinophilic to amphophilic cytoplasm. Anisocytosis, anisokaryosis, and anaplasia were moderate to high, while pleomorphism was moderate. Up to 6 mitoses per 40x power field were observed. Neoplastic cells invaded the perineurium and endoneurium of nerves within the masses (Figures 2 and 3). Affected nerves contained large areas of necrosis with dilatation, vacuolation and fragmentation of myelin sheaths as well as spheroids, deposits of fibrin, infiltrates of neutrophils and lymphocytes, and foci of acute hemorrhage. Neural necrosis extended into the perineural neoplastic tissue, where it was accompanied by prominent infiltration of degenerate neutrophils. Neoplastic cells were present in the perineurium and endoneurium as well. Intralesional within the endoneurium and neoplastic tissue, particularly in areas of necrosis, were syncytia and intranuclear inclusion bodies. These inclusions were predominantly basophilic and filled the nucleus, but eosinophilic inclusions surrounded by a clear halo were noted as well (Figure 3). They were found within syncytia and, presumably, neoplastic cells. Similar infiltrates of neoplastic cells along with fewer well differentiated lymphocytes and plasma cells were present in the spinal cord and root nerves, involving the meninges with a diffuse pattern and neural tissue with a perivascular and multifocal distribution. In the spinal cord, both the white and grey matter was affected (Figure 3). Cerebral meninges were also mildly infiltrated, but predominantly with well differentiated lymphocytes and plasma cells; neoplastic round cells were rare in this location. Neoplastic infiltrates in the retrobulbar mass and adrenal gland caused loss of architecture (Figure 2) and invaded adjacent soft tissues including the skin, adipose tissue and skeletal muscle. Thrombosis was observed in the right eyelid. Other microscopic findings were cataracts in left eye, axonal degeneration in a peripheral skeletal muscle nerve, nodular acinar pancreatic hyperplasia, prostatic hyperplasia, moderate glomerulosclerosis. Additional gross and microscopic findings are summarized in Appendix 3.

PM-9 was a 696-grams male in a good body condition. This mink presented corneal opacity in left eye, and mild thickening of the nictitating membrane. A marked bilateral hemothorax was present, and both lungs were multifocally reddish in color. A mass 0.5 cm diameter was observed in the diaphragmatic lobe of the left lung. This mink had mild to moderate splenomegaly, with a red splenic mass of 0.5 cm in diameter. A cystic mass 1.5 in diameter was also noted in the left liver lobe. A subcutaneous preputial mass measuring 1x0.5x0.3 cm, and mild generalized

lymphadenomegaly were also observed. The adrenal glands contained pale foci less than 1 mm in diameter.

Microscopically, the main disease processes and lesions included pulmonary adenocarcinoma, severe membranous glomerulonephritis, severe chronic diffuse granulomatous lymphadenitis, biliary cystadenoma, and preputial gland cell hyperplasia and cystadenomas with focal malignant transformation and purulent preputial adenitis. Other potential relevant lesions included moderate to marked meningeal mineralization in the lumbar and thoracic spinal cord, mild multifocal spongiosis in the brain, axonal vacuolar degeneration in the thoracic spinal cord and sciatic nerve, as well as nodular hyperplasia of adrenocortical cells, pancreatic acinar and ductal cells and splenic tissue, mild multifocal fibrosis and/or interstitial lymphoplasmacytic nephritis and glomerulosclerosis. Other gross and microscopic findings are summarized in Appendix 3.

Immunohistochemical findings

Positive immunolabeling for the B cell marker CD20 was consistently observed in neoplastic cells in the perineural masses and endoneurium of intra-tumoral nerves (Figure 3). Labeling most notably involved the membrane. No labeling of neoplastic cells was observed for CD3 (Figure 3). Therefore, the lymphoma was classified as a B-cell lymphoma.

Transmission electron microscopy (TEM)

Transmission electron microscopy detected particles approximately 150 nm in diameter in the perineural lymphoma identified in PM-1 (Figure 4). Some of these were similar to empty nucleocapsids while others resembled nucleocapsids containing packaged DNA, and both were compatible with herpesviral particles (Ryner et al., 2006).

DISCUSSION

Two different novel γ-HV sequences were identified in 12 samples from four unrelated adult captive European mink (17.3%, 4/23) that, based on amino acid identities and phylogeny, could be considered novel HV species (MuGHV-2 and MuGHV-3). The prevalence rate should be interpreted with care, once no housekeeping genes were amplified to test the integrity of the DNA present in the samples. This is, to the authors' knowledge, the first report of HV in European mink, expanding the host range of HV infections in mustelids. Other γ-HV species have been previously described in mustelids (King et al., 2004, Tseng et al., 2012, Dalton et al.,

2017), occasionally identified in lesions such as oral ulcerations and plaques (Tseng et al., 2012), and skin ulcers (Gagnon et al., 2011). Nevertheless, this is the first description of γ-HV potentially associated with neoplasms in mustelids.

The two γ-HV-infected European minks with available tissues for histopathology (PM-1 and LM/PM-9) had several neoplasms, including B-cell lymphoma (n=1), pulmonary adenocarcinoma (n=1), biliary cystadenoma (n=1) and preputial cystadenoma (n=1). To the authors' knowledge, these are the first neoplasms described in this species. Age and infectious disease and inbreeding may have played a role in the development of neoplasm. The influence of other factors that may also be implicated, such as environmental contamination or inbreeding, was not assessed. In other carnivore species, for instance the California sea lion (*Zalophus californianus*), collaborative studies showed that certain neoplasms (urogenital carcinoma) were associated with genotype, but also with HV and persistent organic pollutants (King et al., 2002; Browning et al., 2015).

In regard to age, both animals with neoplasms and HV-infection (PM-1 and LM/PM-9) were considered to be of advanced age for the species (over nine years old). The oldest recorded free-ranging European mink was five years old; however, captive animals can reach ten years of age (Mañas et al., 2016a). The nodular acinar pancreatic hyperplasia, prostatic hyperplasia and glomerulosclerosis observed in PM-1, as well as nodular acinar and ductal pancreatic hyperplasia, and nodular splenic hyperplasia in LM/PM-9 were possibly related to aging. Aging should be considered an immunosuppression factor per se (Marchioni & Berzero, 2015), capable of facilitating neoplasm development.

The European mink with neoplasms - PM-1 and LM/PM-9 – were infected with gammaherpesviruses MuGHV-2 and MuGHV-3, respectively. HV-compatible particles were observed by TEM in a B-cell lymphoma with neural tissue tropism of PM-1, in which intratumoral syncytia and intranuclear inclusion bodies characteristic of herpesviruses were noted. Noteworthy, viruses have been associated with approximately 15% to 20% of human cancers worldwide (Parkin et al., 2006; Boccardo & Villa, 2007). Several γ-HV are oncogenic viruses. For instance, Epstein–Barr virus (*Human gammaherpesvirus 4*) has been etiologically associated with a broad range of lymphoproliferative lesions and B-, T- and NK-cell malignant lymphomas in humans (Shannon-Lowe et al., 2017), including B-cell lymphoma in elderly

populations, possibly associated with immunosuppression due to aging (El Jamal, 2014; Castillo et al., 2016). Kaposi sarcoma-associated HV (syn. *Human gammaherpesvirus 8*) is associated with Kaposi's sarcoma and lymphoproliferative disorders in humans (Du et al., 2007). In wild mammals, γ-HVs have been implicated in the pathogenesis of several neoplastic diseases, including urogenital carcinoma or multicentric B-cell lymphoblastic lymphoma in California sea lion (Lipscomb et al., 2000; Venn-Watson et al., 2012; Browning et al., 2015). Gammaherpesvirus-associated lymphoproliferative disease has been observed in captive non-human primates of the family Callitrichidae (Ramer et al., 2000). The experimental inoculation of γ-HV saimiri herpesvirus in three-striped night monkeys (*Aotus trivirgatus*) induced acute lymphocytic leukemia (Melendez et al., 1971), while Epstein-Barr virus inoculation caused lymphoma in cotton-top tamarins (*Saguinus oedipus*) (Miller et al., 1977). The herpesviruses identified in both mink, particularly in PM-1, may have been involved in the etiopathogenesis of the neoplasms found. Conversely, the detection of γ-HVs in several tissues from infected animals presenting neoplasms could have been caused by viral reactivation from latency, triggered by, among other causes, immunosuppression (which could be associated with the presence of neoplasms), given that γ-HVs become latent in lymphoid cells (Roizmann et al., 1992).

In the domestic ferret, a species closely related to the European mink, lymphomas are common spontaneous malignancies. Healthy ferrets experimentally inoculated with non-cellular extracts from ferrets with lymphoma also developed this neoplasm, which reinforces the potential role of infectious agents in the horizontal transmission of lymphomas in this species (Erdman et al., 1995). The role of *Aleutian mink disease virus* and retrovirus infection has been suggested (Erdman et al., 1992). Unfortunately, due to economic constraints, the potential role of retroviruses in European minks has not been assessed yet.

Inbreeding is another factor that could partially explain the observed neoplasms. The French and Spanish European minks appear to be highly inbred (Maran et al., 2016), and it would be interesting to know if these highly genetically uniform populations are more prone to neoplasia. For instance, the loss or lack of major histocompatibility complex (MHC) diversity, known to reduce immune response effectiveness, is postulated to contribute to the successful spread of the devil facial tumour disease of Tasmanian devils (*Sarcophilus harrisii*) (Siddle et al., 2007). The association between neoplasm (urogenital carcinoma) and inbreeding has also been identified in California sea lion (Acevedo-Whitehouse et al., 2003).

The neurological clinical signs – mainly incoordination and rear limb weakness, presented by three of the four HV-positive animals (PM-1, PM-8, LM/PM-9, all over 9 years of age) were initially considered typical signs of weakness or aging-related degenerative disorders. The microscopic lesions described in the peripheral and central nervous systems of two of the examined animals potentially explain the observed neurological signs: peripheral and central nervous system B-cell lymphomas, axonal degeneration, and peripheral skeletal muscle nerves axonal degeneration (PM-1), and brain spongiosis, and spinal cord and sciatic nerve axonal vacuolar degeneration (LM/PM-9). The spongiosis and axonal degeneration observed in LM/PM-9 could be associated with metabolic (e.g., renal encephalopathy) and/or toxic disorders. Noteworthy, LM/PM-9 had severe glomerulonephritis, mild interstitial lymphoplasmacytic nephritis, glomerulosclerosis and azotemia, with high urea (410 mg/dl) and creatinine levels (1.44 mg/dl). These were elevated when compared with the reference values described in other mustelid, the ferret: 11-42 mg/dl and 0.2-1 mg/dl, respectively (Carpenter & Marion, 2017) and the remaining European minks analyzed in this study (data not shown), which could explain the incoordination signs. No reference values are available for European mink.

Interestingly, the MuGHV-2 found in case PM-1 presented neural tissue tropism, with HV particles observed in a perineural mass, and similarly, LM/PM-9 samples of brain, spinal cord, peripheral nerve (sciatic nerve and brachial plexus) were positive to MuGHV-3. Both animals had incoordination. The etiology of the neuritis in the B-cell lymphoma of PM-1 is unclear; it could have been due to secondary inflammation associated with the local necrosis or a direct response against herpesviral infection. Some γ-HVs have marked neurotropism, such as *Human herpesvirus 4*/ Epstein–Barr virus and *Human herpesvirus 4*/Kaposi's sarcoma-associated HV (KSHV) (El Jamal et al., 2014; Tso et al., 2016). For instance, Epstein–Barr virus has been suggested to cause CNS damage by parainfectious and direct virus-related mechanisms in humans (e.g., meningitis, encephalitis and lymphoma) (El Jamal et al., 2014). Thus, it is not possible to exclude HVs as the potential causative agents of the nervous clinical signs observed in these infected mink. Cataracts, corneal melanosis, focal granulomatous conjunctivitis in left eye, and protrusion of and periocular mass around the right eye observed in PM-1 may have contributed to its impaired vision. All mink were seronegative to two other viral agents that could also cause neurological clinical signs and/or impaired vision: *Aleutian mink disease virus* (Hadlow, 1982; Dyer et al., 2000), and canine distemper (Summers et al., 1984). Histopathologic

evidence of infection with *Toxoplasma gondii*, *Encephalitozoon* spp. or *Sarcocystis neurona* was not observed.

One of the novel European mink γ-HVs (Mu-GHV3) was detected in an antemortem oral swab (LM-9), suggesting that viral shedding occurs in infected European minks and, therefore, that horizontal HV transmission through oral secretions could be possible. Such characteristic has been previously identified in γ-HV viruses; Epstein–Barr virus is commonly transmitted via saliva (Marchioni & Berzero, 2015), and other γ-HVs have been detected in sea otter oral mucosal ulcers and plaques (Tseng 2012), and in oral tissue and swabs samples from northern elephant seals (*Mirounga angustirostris*) (Goldstein et al., 2006). None of the mink in this study has oral ulcers. Transmission can be enhanced in captivity as close confinement leads to a higher contact rate between animals and stress-related immunosuppression (Tseng et al., 2012). Interestingly, one of the infected European minks (LM/PM-9) had lesions compatible with chronic stress (bilateral nodular hyperplasia of adrenocortical cells), which could reactivate latent γ-HV in the lymphoid tissue (Roizmann et al., 1992; Lam et al., 2013).

Three of the HV-infected European minks were captured in the Ebro River basin (PM-4, PM-8 and LM/PM-9). The fourth one (PM-1) was born in Pont de Suert in 2006. Herpesvirus can cause lifelong infections (Roizmann et al., 1992); therefore, it was not possible to establish if these animals became infected during their stay in the captive breeding center (the virus was detected when they had already been in captivity for several years) or already carried the virus when they joined the collection. As several European mink conservation programs involving species restoration and reintroduction use animals bred in captivity (Mañas et al., 2001), future studies should investigate whether these HVs are present in wild European mink populations. Due to the fact that several HV infections predispose the host to secondary bacterial infections (Cabello et al., 2013), and considering the small size of the European mink population, the authors believe that monitoring for these viruses should be considered when implementing conservation strategies including translocations, as has been advised for other species, e.g., the Darwin's fox (*Lycalopex fulvipes*) (Cabello et al., 2013).

CONCLUSIONS

This is the first report of HV in European minks. Four European minks were positive to one of the two identified novel herpesviruses: *Mustelid gammaherpesvirus 2* (MuGHV-2) and *Mustelid*

gammaherpesvirus 3 (MuGHV-3). Several neoplasms, including B-cell lymphoma, adenocarcinoma and biliary and preputial cystadenoma, as well as neurological signs, were observed in some of the γ-HV-infected European minks. Aside from the B-cell lymphoma case potentially associated with MuGHV-2, the relationship between γ-HV infection and the remaining lesions is unclear.

This study contributes to the conservation of European minks by expanding the current knowledge on the viral diseases affecting this species. Additional research is needed to establish the prevalence of these novel γ-HVs in free-ranging European mink populations, and to investigate their pathogenicity and the role of herpesvirus and other potential cofactors in the neoplasms detected in this particular European mink captive breeding population. This information will be critical to take more scientifically based decisions and adopt management techniques for the conservation of this endangered species, as well as to determine if infected captive bred European minks could be released into the wild without negatively impacting the species' conservation.

Acknowledgements

We thank the Pont de Suert Captive Breeding Center staff for their assistance and for providing data and audiovisual information on the studied animals and Lene C. Hermansen (Imaging Center, Norwegian University of Life Sciences) for the TEM analysis. We also thank Francesc Mañas (Department of Environment, Generalitat de Catalunya) and Madis Podra (European Mink Association) for their support and interest in this project, and for providing the information regarding the studied animals, and Francisco Fernandez Rivera, Head of the Environmental management in Forestal Catalana, for authorizing this study. Ana Carolina Ewbank receives a doctoral-fellowship from the São Paulo Research Foundation (FAPESP, process number 2018/20956-0). Carlos Sacristán is a recipient of a post-doctoral fellowship by the FAPESP (process number 2018/25069-7). This study was funded by the Innovation Initiative Grant (IIG) and by donors of the Edinburgh Fund (University of Edinburgh).

Conflict of Interest Statement: the authors declare no conflict of interest.

Data Availability Statement: The data that supports our findings are available in the manuscript and in the supplementary material.

REFERENCES

Acevedo-Whitehouse, K., Gulland, F., Greig, D., & Amos, W. (2003). Inbreeding: disease susceptibility in California sea lions. *Nature*, *422*, 35. https://doi.org/10.1038/422035a

Banks, M., King, D. P., & Daniells, C. (2002). Partial characterization of a novel gammaherpesvirus isolated from a European badger (*Meles meles*). *Journal of General Virology*, *83*, 1325–1330. https://doi.org/ 10.1099/0022-1317-83-6-1325

Bodewes, R., Ruiz-Gonzalez, A., Schapendonk, C. M., van den Brand, J. M., Osterhaus, A.D., & Smits, S. L. (2014). Viral metagenomic analysis of feces of wild small carnívores. *Virology Journal*, *11*, 89. https://doi.org/ 10.1186/1743-422X-11-89

Boccardo, E., & Villa, L. L. (2007). Viral origins of human cancer. *Current Medicinal Chemistry*, *14*, 2526–2539. https://doi.org/10.2174/092986707782023316

Browning, H. M., Gulland, F. M. D., & Hammond, J. A. (2015). Common cancer in a wild animal: the California sea lion (*Zalophus californianus*) as an emerging model for carcinogenesis. *Philosophical Transactions of the Royal Society B*, *370*, 1673. https://doi.org/10.1098/rstb.2014.0228.

Cabello, J., Esperón, F., Napolitano, C., Hidalgo, E., Dávila, J. A., & Millán, J. (2013). Molecular identification of a novel gammaherpesvirus in the endangered Darwin's fox (*Lycalopex fulvipes*). *Journal of General Virology*, *94*, 2745–2749. https://doi.org/10.1099/vir.0.057851-0.

Carpenter, J. W., & Marion, C. (2017). *Exotic Animal Formulary* (5th ed.). Philadelphia, PA: Saunders.

Castillo, J. J., Beltran, B. E., Miranda, R. N., Young, K. H., Chavez, J. C., & Sotomayor, E. M. (2016). EBV-positive diffuse large B-cell lymphoma of the elderly: 2016 update on diagnosis, risk-stratification, and management. *American Journal of Hematology*, *91*, 529-537. https://doi.org/10.1002/ajh.24370

Dalton, C. S., van de Rakt, K., Fahlman, Å., Ruckstuhl, K., Neuhaus, P., Popko, R., Kutz, S., & van der Meer, F. (2017). Discovery of herpesviruses in Canadian wildlife. *Archives of Virology*, *162*, 449-456

Dandár, E., Szabó, L., & Heltai, M. (2010). PCR screening of mammalian predators (Carnivora) for adenoviruses and herpesviruses: the first detection of a mustelid herpesvirus in Hungary. *Magyar Allatorvosok Lapja*, *132*, 302-308.

Du, M. -Q., Bacon, C. M., & Isaacson, P. G. (2007). Kaposi sarcoma-associated herpesvirus/human herpesvirus 8 and lymphoproliferative disorders. *Journal of Clinical Pathology*, *60*, 1350-1357.

Dyer, N. W., Ching, B., & Bloom, M. E. (2000). Nonsuppurative meningoencephalitis associated with Aleutian mink disease parvovirus infection in ranch mink. *Journal of Veterinary Diagnostic Investigation*, *12*, 159–162. https://doi.org/10.1177/104063870001200212

Ehlers, B., Dural, G., Yasmum, N., Lembo, T., de Thoisy, B., Ryser-Degiorgis, M. P., Ulrich, R. G., & McGeoch, D. J. (2008). Novel mammalian herpesviruses and lineages within the Gammaherpesvirinae: cospeciation and interspecies transfer. *Journal of Virology*, *82*, 3509–3516. https://doi.org/10.1128/JVI.02646-07.

El Jamal, S., Li, S., Bajaj, R., Wang, Z., Kenyon, L., Glass, J., Pang, C.S., Bhagavathi, S., Peiper, S. C., & Gong, J. Z. (2014). Primary central nervous system Epstein–Barr virus-positive diffuse large B-cell lymphoma of the elderly: a clinicopathologic study of five cases. *Brain Tumor Pathology*, *31*, 265–273. https://doi.org/10.1007/s10014-013-0173-x

Erdman, S. E., Moore, F. M., Rose, F. M., & Fox, J. G. (1992). Malignant lymphoma in ferrets: clinical and pathological findings in 19 cases. *Journal of Comparative Pathology*, *106*, 37–47. https://doi.org/10.1016/0021-9975(92)90066-4

Erdman, S. E., Reimann, K. A., Moore, F. M., Kanki, P. J., Yu, Q. C., & Fox, J. G. (1995). Transmission of a chronic lymphoproliferative syndrome in ferrets. *Laboratory Investigation; a Journal of Technical Methods and Pathology*, *72*, 539-546.

Ferrer, M. (2014). Life Lutreola Spain (2014-2018). Retrieved from http://ec.europa.eu/environment/life/project/Projects/index.cfm?fuseaction=search.dspPage&n_proj_id=4908

Fournier-Chambrillon, C., Aasted, B., Perrot, A., Pontier, D., Sauvage, F., Artois, M., Cassiède, J. M., Chauby, X., Dal Molin, A., Simon, C., & Fournier, P. (2004). Antibodies to Aleutian mink disease parvovirus in free-ranging European mink (*Mustela lutreola*) and other small carnivores

from southwestern France. *Journal of Wildlife Diseases*, *40*, 394-402. https://doi.org/10.7589/0090-3558-40.3.394

Gagnon, C. A., Tremblay, J., Larochelle, D., Music, N., & Tremblay, D. (2011). Identification of a novel herpesvirus associated with cutaneous ulcers in a fisher (*Martes pennanti*). *Journal of Veterinary Diagnostic Investigation*, *23*, 986–990. https://doi.org/10.1177/1040638711418615.

Goldstein, T., Lowenstine, L. J., Lipscomb, T. P., Mazet, J. A., Novak, J., Stott, J. L., & Gulland, F. M., (2006). Infection with a novel gammaherpesvirus in northern elephant seals (*Mirounga angustirostris*). *Journal of Wildlife Diseases*, *42*, 830–835. https://doi.org/10.7589/0090-3558-42.4.830

Goldstein, T., Gill, V. A., Tuomi, P., Monson, D., Burdin, A., Conrad, P. A., Dunn, J. L., Field, C., Johnson, C., Jessup, D. A., Bodkin, J., & Doroff, A. M. (2011). Assessment of clinical pathology and pathogen exposure in sea otters (*Enhydra lutris*) bordering the threatened population in Alaska. *Journal of Wildlife Diseases*, *47*, 579-592. https://doi.org/10.7589/0090-3558-47.3.579

Gorham, J. R., Hartsough, G. R., & Burger, D. (1998). An epizootic of pseudorabies in ranch mink. *Scientifur*, *22*, 243-245.

Guzmán, D. S. M., Carvajal, A., García-Marín, J. F., Ferreras, M. C., Pérez, V., Mitchell, M., Urra, F., & Ceña, J. C. (2008). Aleutian disease serology, protein electrophoresis, and pathology of the European mink (*Mustela lutreola*) from Navarra, Spain. *Journal of Zoo and Wildlife Medicine*, *39*, 305–313. https://doi.org/10.1638/2006-0033.1

Hadlow, W. J. (1982). Ocular lesions in mink affected with Aleutian disease. *Veterinary Pathology*, *19*, 5–15. https://doi.org/10.1177/030098588201900103

Huff, J. L., & Barry, P. A. (2003). B-Virus (*Cercopithecine herpesvirus*1) infection in humans and macaques: potential for zoonotic disease. *Emerging Infectious Diseases*, *9*, 246-250. https://doi.org/10.3201/eid0902.020272

ICTV (International Committee on Taxonomy of Viruses). (2017). Virus Taxonomy: The Classification and Nomenclature of Viruses. Online (9th) Report of the ICTV. Email ratification 2017 (MSL #31). Retrieved from https://talk.ictvonline.org/ictv-reports/ictv_online_report/

Kent, A., Ehlers, B., Mendum, T., Newman, C., Macdonald, D. W., Chambers, M., & Buesching, C. D. (2018). Genital tract screening finds widespread infection with Mustelid Gammaherpesvirus 1 in the European badger (*Meles meles*). *Journal of Wildlife Diseases*, *54*, 133-137. https://doi.org/10.7589/2016-12-274

King, D. P., Hure, M. C., Goldstein, T., Aldridge, B. M., Gulland, F. M., Saliki, J. T., Buckles, E. L., Lowenstine, L. J., & Stott, J. L. (2002). Otarine herpesvirus-1: a novel gammaherpesvirus associated with urogenital carcinoma in California sea lions (*Zalophus californianus*). *Veterinary Microbiology*, *86*, 131-137. https://doi.org/10.1016/s0378-1135(01)00497-7

King, D. R., Mutukwa, N., Lesellier, S., Cheeseman, C., Chambers, M. A., & Banks, M. (2004). Detection of Mustelid herpesvirus-1 infected European badgers (*Meles meles*) in the British Isles. *Journal of Wildlife Diseases*, *40*, 99–102. https://doi.org/10.7589/0090-3558-40.1.99

Kumar, S., Stecher, G., Tamura, K. (2016). MEGA7: Molecular Evolutionary Genetics Analysis version 7.0 for bigger datasets. *Molecular Biology and Evolution*, *33*, 1870–1874. https://doi.org/10.1093/molbev/msw054

Lam, L., Garner, M. M., Miller, C. L. (2013). A novel gammaherpesvirus found in oral squamous cell carcinomas in sun bears (*Helarctos malayanus*). Journal *of Veterinary Diagnostic Investigation*, *25*, 99–106.

Lipscomb, T. P., Scott, D. P., Garber, R. L., Krafft, A. E., Tsai, M. M., Lichy, J. H., Taubenberger, J. K., Schulman, F. Y., & Gulland, F. M. (2000). Common metastatic carcinoma of California sea lions (*Zalophus californianus*): evidence of genital origin and association with novel gammaherpesvirus. *Veterinary Pathology*, *37*, 609–617. https://doi.org/10.1354/vp.37-6-609

Liu, H., Li, X. T., Hu, B., Deng, X. Y., Zhang, L., Lian, S. Z., Zhang, H. L., Lv, S., Xue, X. H., Lu, R. G., Shi, N., Yan, M. H., Xiao, P. P., & Yan, X. J. (2017). Outbreak of severe pseudorabies virus infection in pig-offal-fed farmed mink in Liaoning Province, China. *Archives of Virology*, *162*, 863-866. https://doi.org/10.1007/s00705-016-3170-7.

Lodé, T., Cormier, J. P., & Le Jacques, D. (2001). Decline in endangered species as an indication of anthropic pressures: the case of European mink *Mustela lutreola* Western population. *Environmental Management*, 28, 727-735. https://doi.org/10.1007/s002670010257

Mañas, S., Ceña, J. C., Ruiz-Olmo, J., Palazón, S., Domingo, M., Wolfinbarger, J. B., & Bloom, M. E. (2001). Aleutian mink disease parvovirus in wild riparian carnivores in Spain. *Journal of Wildlife Diseases*, *37*, 138-144. https://doi.org/10.7589/0090-3558-37.1.138

Mañas, S., Gómez, A., Asensio, V., Palazón, S., Pŏdra, M., Casal, J., & Ruiz-Olmo, J. (2016a). Demographic structure of three riparian mustelid species in Spain. *European Journal of Wildlife Research*, *62*, 119-129. https://doi.org/10.1007/s10344-015-0982-9

Mañas, F., Gómez, A., Asensio, V., Palazón, S., Podra, M., Alarcia, O.E., Ruiz-Olmo, J., & Casa, J. (2016b). Prevalence of antibody to aleutian mink disease virus in European mink (*Mustela lutreola*) and american mink (*Neovison vison*) in Spain. *Journal of Wildlife Diseases*, *52*, 22–32. https://doi.org/10.7589/2015-04-082

Maran, T., Skumatov, D., Gomez, A., Põdra, M., Abramov, A. V., & Dinets, V. (2016). *Mustela lutreola*. The IUCN Red List of Threatened Species 2016. Retrieved from https://www.iucnredlist.org/species/14018/45199861

Marchioni, E., & Berzero, G. (2015). Viral Infections of the Nervous System, In A. Sghirlanzoni, G. Lauria, L. Chiapparini (Eds.), *Prognosis of Neurological Diseases*. (pp. 75-92) Milan, Italy: Springer-Verlag Italia. https://doi.org/10.1007/978-88-470-5755-5

Melendez, L. V., Hunt, R. D., Daniel, M. D., Blake, B. J., & Garcia, F. G. (1971). Acute lymphocytic leukemia in owl monkeys inoculated with herpesvirus saimiri. *Science*, *171*, 1161–1163. https://doi.org/10.1126/science.171.3976.1161

Miller, G., Shope, T., Coope, D., Waters, L., Pagano, J., Bornkamn, G., & Henle, W. (1977). Lymphoma in cotton-top marmosets after inoculation with Epstein-Barr virus: tumor incidence, histologic spectrum antibody responses, demonstration of viral DNA, and characterization of viruses. *Journal of Experimental Medicine, 145*, 948–967. https://doi.org/10.1084/jem.145.4.948

Parkin, D. M. (2006). The global health burden of infection-associated cancers in the year 2002. *International Journal of Cancer*, *118*, 3030–3044. https://doi.org/10.1002/ijc.21731

Philippa, J., Fournier-Chambrillon, C., Fournier, P., Schaftenaar, W., van de Bildt, M., van Herweijnen, R., Kuiken, T., Liabeuf, M., Ditcharry, S., Joubert, L., Bégnier, M., & Osterhaus, A. (2008). Serologic survey for selected viral pathogens in free-ranging endangered European mink (*Mustela lutreola*) and other mustelids from south-western France. *Journal of Wildlife Diseases*, *44*, 791–801. https://doi.org/10.7589/0090-3558-44.4.791

Quiroga, M. I., López-Peña, M., Vázquez, S., & Nieto, J. M. (1997). Distribution of Aujeszky's disease virus in experimentally infected mink (*Mustela vison*). *Deutsche tierärztliche Wochenschrift*, *104*, 147-150.

Ramer, J. C., Garber, R. L., Steele, K. E., Boyson, J. F., O'Rourke, C., & Thomson, J. A. (2000). Fatal lymphoproliferative disease associated with a novel gammaherpesvirus in a captive population of common marmosets. *Comparative Medicine*, *50*, 59-68.

Reading, M. J., & Field, H. J. (1999). Detection of high levels of canine herpes virus 1 neutralising antibody in kennel dogs using a novel serum neutralisation test. *Research in Veterinary Science*, *66*, 273-275. https://doi.org/10.1053/rvsc.1998.0222

Reimer, D. C., & Lipscomb, T. P. (1998). Malignant seminoma with metastasis and herpesvirus infection in a free-living sea otter (*Enhydra lutris*). *Journal of Zoo and Wildlife Medicine*, *29*, 35-39.

Roizmann, B., Desrosiers, R. C., Fleckenstein, B., Lopez, C., Minson, A. C., & Studdert, M. J. (1992). The family *Herpesviridae*: an update. *Archives of Virology*, *123*, 425–449. https://doi.org/10.1007/bf01317276

Ryner, M., Strömberg, J. O., Söderberg-Nauclér, C., & Homman-Loudiyi, M. (2006). Identification and classification of human cytomegalovirus capsids in textured electron micrographs using deformed template matching. *Virology Journal*, *3*, 57. https://doi.org/10.1186/1743-422X-3-57

Shannon-Lowe, C., Rickinson, A. B., & Bell, A. I. (2017). Epstein–Barr virus-associated lymphomas. *Philosophical Transactions of the Royal Society B*, *372*, 20160271. https://doi.org/10.1098/rstb.2016.0271

Siddle, H. V., Kreiss, A., Eldridge, M. D., Noonan, E., Clarke, C. J., Pyecroft, S., Woods, G. M., & Belov, K. (2007). Transmission of a fatal clonal tumor by biting occurs due to depleted MHC diversity in a threatened carnivorous marsupial. *Proceedings of the National Academy of Sciences of the United States of America*, *104*, 16221–16226. https://doi.org/10.1073/pnas.0704580104

Sin, Y. W., Annavi, G., Dugdale, H. L., Newman, C., Burke, T., & MacDonald, D. W. (2014). Pathogen burden, co-infection and major histocompatibility complex variability in the European badger (*Meles meles*). *Molecular Ecology*, *23*, 5072–5088. https://doi.org/10.1111/mec.12917.

Summers, B., Greisen, H., & Appel, M. J. (1984). Canine distemper encephalomyelitis: variation with virus strain. *Journal of Comparative Pathology*, *94*, 65-75. https://doi.org/10.1016/0021-9975(84)90009-4

Tseng, M., Fleetwood, M., Reed, A., Gill, V. A., Harris, R. K., Moeller, R. B., Lipscomb, T. P., Mazet, J. A., & Goldstein, T. (2012). Mustelid Herpesvirus-2, a novel herpes infection in northern sea otters (*Enhydra lutris kenyoni*). *Journal of Wildlife Diseases*, *48*, 181–185. https://doi.org/10.7589/0090-3558-48.1.181

Tso, F. Y., Sawyer, A., Kwon, E. H., Mudenda, V., Langford, D., Zhou, Y., West, J., & Wood, C. (2016). Kaposi's Sarcoma–Associated Herpesvirus Infection of Neurons in HIV-Positive Patients. *The Journal of Infectious Diseases*, *215*, 1898-1907. https://doi.org/10.1093/infdis/jiw545.

VanDevanter, D. R., Warrener, P., Bennett, L., Schultz, E. R., Coulter, S., Garber, R. L., & Rose, T. M. (1996). Detection and analysis of diverse herpesviral species by consensus primer PCR. *Journal of Clinical Microbiology*, *34*, 1666–1671.

Venn-Watson, S., Benham, C., Gulland, F. M., Smith, C. R., St Leger, J., Yochem, P., Nollens, H., Blas-Machado, U., Saliki, J., Colegrove, K., Wellehan, J. F. Jr., & Rivera, R. (2012). Clinical relevance of novel Otarine herpesvirus-3 in California sea lions (*Zalophus californianus*): Lymphoma, esophageal ulcers, and strandings. *Veterinary Research*, *43*, 85. https://doi.org/10.1186/1297-9716-43-85

Wang, G., Du, Y., Wu, J. Q., Tian, F. L., Yu, X. J., & Wang, J. B. (2018). Vaccine resistant pseudorabies virus causes mink infection in China. *BMC Veterinary Research*, *14*, 20. https://doi.org/10.1186/s12917-018-1334-2

Widén, F., Das Neves, C. G., Ruiz-Fons, F., Reid, H. W., Kuiken, T., Gavier-Widén, D., & Kaleta, E. F. (2012). *Herpesvirus Infections*. In D. Gavier-Widén, P. J. Duff, & A. Meredith. (Eds.), *Infectious Diseases of Wild Mammals and Birds in Europe*. (pp. 3–36). Ames: Blackwell Publishing Ltd. https://doi.org/10.1002/9781118342442

637 **Table 1.** Herpesviruses infections described in the family Mustelidae.

Species	HV name in the article	GenBank access nº.	Lesions attributable to herpesvirus	PCR prevalence	Tissue	Country	Author
European badger (*Meles meles*)	Mustelid herpesvirus 1 (MusHV-1, γ-HV)	AF376034 AY050215 AF275656	Cytopathic effect on badger' pulmonary fibroblasts	Single case	Pulmonary fibroblasts	UK	Banks et al. (2002)
	Mustelid herpesvirus-1 (MusHV-1, γ-HV)	Not provided	Not described	95% (18/19) 100% (10/10)	Blood Blood	UK Ireland	King et al. (2004)
	Mustelid herpesvirus-1 (MusHV-1, γ-HV)	GU799569	Not reported (detected in a road-kill animal)	Single case		Hungary	Dandár et al. (2010)
	Mustelid herpesvirus-1 (MusHV-1, γ-HV)	Not provided	Not described	98.1% (354/361)	Blood	UK	Sin et al. (2014)
	Mustelid gammaherpesvirus 1	AF275657	Not described	Single case	Lung	Not described	Unpublished
	Mustelid alphaherpesvirus 1	MF042164	Not described	Single case	Mediastinal lymph node	France	Unpublished
	Mustelid gammaherpesvirus-1 (MusGHV-1)	Not provided	Not detected	55% (54/98)	Genital swabs	UK	Kent et al. (2018)
Northern sea otter (*Enhydra lutris kenyoni*)	Mustelid herpesvirus-2 (MusHV-2, γ-HV)	GU979535	Presence of ulcers or pale raised plaques on the lingual, gingival, oral, esophageal and labial mucosa: epithelial hyperplasia and hyperkeratosis, often with epithelial cell degeneration and ulceration, and presence of eosinophilic intranuclear inclusion	46% (13/28)	Skin biopsies	United States	Tseng et al. (2012)

			bodies) Apparently healthy animal	34% (21/62)	nasal swabs	United States	
Oriental small-clawed otter (*Aonyx cinerea*)	Oriental small-clawed otter gammaherpesvirus (γ-HV)	FJ797657	Not described	Single case	Not described	Hungary	Unpublished
Captive fisher (*Martes pennanti*)	Fisher herpesvirus (FiHV, γ-HV)	HM579931	Multiple skin ulcers on the muzzle and plantar pads (thickened epidermis with increased numbers of koilocytes, perinuclear vacuolation, nuclear hypertrophy, pale amphophilic intranuclear inclusion bodies, and basophilic pseudoinclusions)	Single case	Skin ulcers	Born in captivity in the Unites States and sent to Canada	Gagnon et al. (2011)
American marten (*Martes americana*)	Marten alphaherpesvirus	KX062131 KX062132 KX062133	Not described	3 cases	Not described	Canada	Dalton et al. (2017)
	Marten betaherpesvirus	KX062129 KX062134 KX062135 KX062136	Not described	4 cases	Not described		
	Marten gammaherpesvirus 1	KX062128	Not described	2 cases	Not described		
	Marten gammaherpesvirus 2	KX062130					
European mink (*Mustela lutreola*)	Mustelid gammaherpesvirus-2	MN082678, MN082679	Basophilic (or eosinophilic, rarely found) inclusion bodies, and syncytia in a multifocal neural and perineural lymphoma.	8.7% (2/23)	Mediastinal B-cell lymphoma and lung	Spain	This work

	Mustelid gammaherpesvirus-3	MN082680	Not detected	8.7% (2/23)	Oral swab, kidney, liver, spleen, bone marrow, brain, spinal cord, sciatic nerve and brachial plexus

638

FIGURES

Figure 1. Maximum likelihood phylogram of the alignment of the obtained deduced amino acid gammaherpesvirus sequences (marked with red dots) and other herpesvirus sequences retrieved from GenBank. *Ictalurid herpesvirus 1* was selected as outgroup. The reliability of the tree was tested by bootstrap analysis with 1,000 replicates, and those bootstrap values lower than 70 were omitted.

Figure 2. Gross and microscopic findings in European mink (*Mustela lutreola*) PM-1: **(A)** Periocular mass (white arrow). Scale bar = 1 centimeter. **(B)** Retrobulbar mass (right eye, black arrow). Scale bar = 1 centimeter. **(C)** Perineural mass along the brachial plexus (black arrows) and mediastinal mass (white arrow). Scale bar = 1 centimeter. **(D)** Mass effacing the left adrenal gland (black arrow). **(E)** Note diffuse infiltration of neoplastic lymphocytes in the perineural tissues and endoneurium of the brachial plexus mass; n = nerves (hematoxylin and eosin). **(F)** Adrenal gland (a) is invaded by lymphoma (delimited with arrowheads) (hematoxylin and eosin).

Figure 3. Microscopic and immunohistochemical findings in European mink (*Mustela lutreola*) PM-1: **(A)** Higher magnification of endoneural (arrows) and perineural lymphoid infiltrates in the brachial plexus mass. Note necrosis of neural tissue (asterisk). **(B)** A higher magnification of neoplastic infiltrates demonstrates neoplastic lymphoblasts (hematoxylin and eosin). **(C)** Note numerous basophilic intranuclear inclusion bodies (red arrowheads) in unidentified cells and syncytia (black arrows) and few eosinophilic intranuclear inclusion bodies surrounded by a clear halo (black arrowhead) in an area of necrosis involving a nerve in the brachial plexus with perineural and neural lymphoma (hematoxylin and eosin). **(D)** Lymphoma involving the spinal cord, particularly the pachymeninges (delimited with black arrowheads) but also the white and grey matter (red arrowheads) (hematoxylin and eosin). **(E)** Note positive immunolabeling for CD20 in perineural and endoneural neoplastic lymphocytes in the brachial plexus mass. **(F)** Neoplastic lymphocytes are not labeled with CD3 antibodies.

Figure 4. Transmission electron microscopy (TEM) of the perineural lymphoma found in European mink (*Mustela lutreola*) PM-1: **(A)** Intracytoplasmic herpesvirus-like particle (red

arrow) after nuclear egression but prior to acquiring the secondary envelopment in the cytoplasm (which leads to the well-known enveloped herpesvirus particles seen on mature virions) and nuclear membrane (yellow arrow), **(B)** Detailed view of the same particle (red arrow) and nuclear membrane (yellow arrow).

Neoplasms and novel gammaherpesviruses in critically endangered captive European minks (*Mustela lutreola*)

Running title: Neoplasms and gammaherpesviruses in European minks

Olga Nicolas de Francisco[1], Fernando Esperón[2], Carles Juan-Sallés[3], Ana Carolina Ewbank[4], Carlos G. das Neves[5], Alberto Marco[6], Elena Neves[2], Neil Anderson[1] and Carlos Sacristán[2,4,*]

[1]The Royal (Dick) School of Veterinary Studies and the Roslin Institute, University of Edinburgh, Roslin, EH25 9RG, UK.

[2]Group of Epidemiology and Environmental Health, Animal Health Research Center (INIA-CISA).Valdeolmos, Madrid, 28130, Spain.

[3]Noah's Path, Elche, Alicante, 03203, Spain.

[4]Laboratory of Wildlife Comparative Pathology, Department of Pathology, School of Veterinary Medicine and Animal Sciences, University of São Paulo, São Paulo, SP, 05508-270, Brazil.

[5]Norwegian Veterinary Institute. Oslo, PO Box 750 Sentrum, Norway.

[6]Departament de Sanitat i d'Anatomia Animals, Facultat de Veterinària, Universitat Autònoma de Barcelona (UAB), Bellaterra-Barcelona, 08193, Spain.

*Corresponding author: Carlos Sacristán, Laboratory of Wildlife Comparative Pathology, Department of Pathology, School of Veterinary Medicine and Animal Sciences, University of São Paulo, São Paulo, SP, Av. Prof. Dr. Orlando Marques de Paiva, 87, 05508-270, Brazil; Tel: +55 11 981 121 073; Email: carlosvet.sac@gmail.com

SUMMARY

The European mink (*Mustela lutreola*) is a riparian mustelid, considered one of the most endangered carnivores in the world. Alpha, beta, and gammaherpesviruses described in mustelids have been occasionally associated with different pathological processes. However, there is no information about the herpesviruses species infecting European minks. In this study, 141 samples of swabs (oral, conjunctival, anal), feces and tissues from 23 animals were analyzed for herpesvirus (HV) using a pan-HV PCR assay. Two different, potentially novel, gammaherpesvirus species were identified in 12 samples from four animals (17.3%), and tentatively named Mustelid gammaherpesvirus-2 (MUGHV-2) and MuGHV-3. Gross examination was performed on dead minks (n=11), while histopathology was performed using available samples from HV-positive individuals (n=2), identifying several neoplasms, including B-cell lymphoma (identified by immunohistochemistry) with intralesional syncytia and intranuclear inclusion bodies characteristic of HV (n=1), pulmonary adenocarcinoma (n=1), and biliary (n=1) and preputial (n=1) cystadenoma, as well as other lesions (e.g., axonal vacuolar degeneration [n=2] and neuritis [n=1]). Viral particles, consistent with HVs, were observed by electron microscopy in the mink with neural lymphoma and inclusion bodies. This is the first description of neoplasms and concurrent gammaherpesvirus infection in European minks. The pathological, ultrastructural and PCR findings (MuGHV-2) in the European mink with lymphoma strongly suggest a potential role for this novel gammaherpesvirus in its pathogenesis, as it has been reported in other HV-infected species with lymphoma. The occurrence of neural lymphoma with intralesional syncytia and herpesviral inclusions is, however, unique among mammals. Further research is warranted to elucidate the potential oncogenic properties of gammaherpesviruses in European mink, and their epidemiology in the wild population.

Keywords: biliary cystadenoma, herpesvirus, lymphoma, lung adenocarcinoma, mustelid, preputial cystadenoma.

INTRODUCTION

The European mink (*Mustela lutreola*) is a critically endangered riparian mustelid with populations in eastern (Ukraine, Russia, Estonia and Romania) and western (south-western France and northern Spain) Europe (Maran et al., 2016). The main factors causing its decline are interspecies competition with the non-native American mink (*Neovison vison*), habitat loss and degradation (pollution), over-hunting, and infectious diseases (e.g., Aleutian mink disease and canine distemper) (Lodé et al., 2001; Maran et al., 2016; Mañas et al., 2016a). Without the implementation of more effective conservation measures, the European mink will very likely soon become extinct in Spain (Ferrer, 2014).

To date, the exposure to, and infection by, several viruses have been studied in wild European minks: *Aleutian mink disease virus* (Mañas et al., 2001; Fournier-Chambrillon et al., 2004; Guzmán et al., 2008; Mañas et al., 2016b), *Canine morbillivirus* (syn. canine distemper virus) (Mañas et al., 2001; Guzmán et al., 2008; Philippa et al., 2008), canine parainfluenza virus (syn. parainfluenza virus type 5 or *Mammalian rubulavirus 5*), canine adenovirus (syn. *Canine mastadenovirus A*), and viruses belonging to the families *Astroviridae*, *Picobirnaviridae*, and *Parvoviridae* subfamily *Parvovirinae* (Bodewes et al., 2014). Nevertheless, in spite of the numerous members of the family *Herpesviridae* of veterinary and public health significance (Huff & Barry, 2003; Widén et al., 2012), to the authors' knowledge, there is no information about herpesviruses (HVs) in European minks. The HVs infecting vertebrates (family *Herpesviridae*) are further subdivided into three subfamilies: *Alphaherpesvirinae*, *Betaherpesvirinae* and *Gammaherpesvirinae* (ICTV, 2017). In other mustelid species, for example the sea otter (*Enhydra lutris*), HV-like intranuclear inclusion bodies along with HV-compatible virions, and exposure to herpesvirus have been described (Reimer & Lipscomb, 1998; Goldstein et al., 2011). Alpha-, beta- and gammaherpesviruses (α-HVs, β-HVs, γ-HVs) were identified in American martens (*Martes Americana*) with no mention to associated disease (Dalton et al., 2017). Only γ-HV infection has been reported in other mustelids: in oral ulcerations and plaques, and nasal secretions of sea otters (Tseng et al., 2012); in ulcerative skin lesions of a captive fisher (*Martes pennanti*) (Gagnon et al., 2011); and in free-living European badgers (*Meles meles*) (Banks et al., 2002; Dandár et al., 2010, Sin et al., 2014), in which a γ-HV has not yet been associated with lesions or clinical disease (King et al., 2004). Finally, the susceptibility to α-HV *Suid alphaherpesvirus 1*, the etiological agent of Aujesky'

disease/pseudorabies (Gorham et al., 1998; Quiroga et al., 1997; Liu et al., 2017; Wang et al., 2018) and the replication of α-HV *Canine herpesvirus-1* in fetal lung cells (Reading & Field, 1999) have been reported in American mink.

The goals of this study were to: (1) survey if HVs are present in a European mink captive population; and (2) describe the clinical and pathological findings with a particular focus on morphological evidence of an association with herpesviral infection.

MATERIALS AND METHODS

Study population and samples

This study was performed on the captive European mink population of the Pont de Suert Captive Breeding Center (Pont de Suert, Lleida, northeastern Spain) which is part of the Spanish Breeding Program. Ethical approval for this study was granted by the R(D)SVS Veterinary Ethical Review Committee (VERC, process number 57.17) and the Government of Catalonia (Wildlife and Plant Service within the Department of Sustainability and Territory).

The European mink samples were obtained from the live animal collection of the Pont de Suert captive collection in September 2017 (identified as LM = live mink) and from the dead mink stored at that center until October 2017 (identified as PM = postmortem mink). All these mink were either originated from Spanish captive breeding centers or captured in the wild, also in Spain. Individual sex, last weight, date and place of birth (when available), origin, and arrival date to Pont de Suert, and date of death or euthanasia are summarized in Appendix 1. All European minks in Pont de Suert tested negative for *Aleutian mink disease virus* and *Canine morbillivirus* antibodies upon their admission to the captive breeding program.

In September 2017, all live adult European mink in the breeding center were anesthetized for routine health check with a combination of intramuscular ketamine (5 mg/kg, Imalgene 100 mg/mL, Merial Laboratorios SA, Barcelona, Spain) and medetomidine (0.1 mg/kg, Domtor, Ecuphar Veterinaria SLU, Barcelona, Spain). Intramuscular atipamezole (0.1 mg/kg, Antisedan, Zoetis SLU, Madrid, Spain) was used to reverse the effects of medetomidine a minimum of 20 minutes after anesthesia had been induced. All animals were individually placed back into their cages after sampling and full recovery. During anesthesia, all mink received a full clinical examination by an experienced veterinarian, which included body condition assessment, skin and hair inspection for ectoparasites, abdominal palpation and general examination of the mucosae,

oral cavity, ears, anal-genital region and feet, and cardiac and pulmonary auscultation. Approximately 2 ml of blood were withdrawn by venipuncture from the cranial vena cava using 21-gauge 3.8-cm needles for hematology, biochemistry (data not shown), and molecular analysis (0.5 mL in a sterile eppendorf). Aside from 0.5 mL of whole blood, sterile oropharyngeal, conjunctival and anal swabs were also collected for molecular analysis, and preserved frozen at -20 ºC. Fresh fecal samples were taken from the cages using a sterile tube and refrigerated for direct observation and egg flotation techniques with zinc sulphate (33%) for endoparasite detection (data not shown) or frozen (-20 ºC) to perform viral DNA detection.

Molecular diagnostics

A total of 141 frozen tissue samples from 23 European minks were analyzed by PCR for HV detection. Anal and conjunctival swabs, blood, and feces from live mink (n=12) and representative tissue samples from carcasses (n=10) (Appendix 2) were submitted for PCR analysis. One additional animal was sampled while alive and after its death (codes LM-9 and PM-9), thus included in both categories (live animal and carcasses, Appendix 2). After a lysis step with lysis buffer (Cell Signaling Technology, MA, USA), DNA extraction was performed by pressure filtration (QuickGene DNA tissue kit S, FujiFilm Life Science, Tokyo, Japan). Initially, a mediastinal neoplastic tissue mass from PM-1 (index case) was analyzed by a nested pan-PCR that amplified a fragment of approximately 215-315 bp of the HV DNA polymerase gene (VanDevanter et al., 1996). A second PCR was performed to amplify a 500 bp fragment of the HV glycoprotein B gene for gammaherpesviruses (Ehlers et al., 2008). In order to explore the presence of the novel HV sequence obtained from the neoplastic tissue, a comprehensive HV screening in tissues and samples from the captive breeding center (both live and dead animals) was performed using the PCR described by Ehlers et al. (2008). All glycoprotein B gene-positive samples were also tested for herpesviral DNA polymerase gene (VanDevanter et al., 1996).

The PCR products of DNA polymerase and glycoprotein B were visualized in 1.5% agarose gel stained with Red Safe® (Ecogen, Spain), and the amplicons of expected size were directly sequenced with sequencing primers TGVseq and IYGseq (DNA polymerase), and 2760s and 2761as (glycoprotein B), respectively described by VanDevanter et al. (1996) and Ehlers et al. (2008). The obtained sequences were compared to those previously published in GenBank using a Blast search, and nucleotide (nt) and deduced amino acid (aa) p-distances were calculated with

MEGA Software 7.0 after editing out the primers (Kumar et al., 2016). After ClustalW alignment of glycoprotein B gene nucleotide sequences by MEGA software 7.0 (Kumar et al., 2016), nt and aa maximum likelihood phylogenetic trees were generated with 1000 bootstrap replicates, including the newly identified HV sequences and 39 other α-, β-, and γ-HVs sequences. *Ictalurid herpesvirus 1* was selected as an outgroup. Sequence information for members of the *Herpesviridae* family was obtained from GenBank.

Gross and microscopic examination

Complete postmortem gross examination was performed in eleven European mink (identified with codes PM-1 through PM-11). Eight of them (PM-2 – PM-8, and PM-10) were prominently autolyzed. Microscopic evaluation was performed on HV-PCR-positive animals with adequate tissue preservation (PM-1 and PM-9), using 10% formalin-fixed tissues embedded in paraffin, sectioned at 5 µm-thick, and stained with hematoxylin and eosin.

Immunohistochemistry

Immunohistochemical analyses were performed in 4 µm-thick paraffin wax-embedded tissue samples of PM-1 using antibodies against CD20 and CD3. Briefly, slides were transferred to a PT-Link Automatic System of DAKO for deparaffinization, rehydration and epitope retrieval. For this last step, slides were treated with acid buffer at pH 6 for 20 min. at 98ºC, and then transferred to distilled water. Endogenous peroxidase was then inhibited with Peroxidase-Blocking Solution (from Dako, Ref.: S2023). Immunostaining was performed on a Dako Autostainer Plus, using procedures, buffers and solutions provided by the fabricant. Briefly, as first antibody, a polyclonal Rabbit Anti- Human CD3 antibody (DAKO. Ref: A0452) and a polyclonal Rabbit Anti- Human CD20 antibody (CULTEK. Ref: PA5-32313) were both incubated for 40 min. at room temperature, diluted 1:100 (CD3) and 1:200 (CD20) in EnVision™ FLEX buffer. After washing, the Rabbit/Mouse EnVision Detection System (Dako Ref.: K5007) was incubated at room temperature for 40 min, at the dilution recommended by the supplier. After washing, slides were incubated for 5 min. in DAB-Chromogen-hydrogen peroxide (Dako K3468), to reveal binding. After washing, slides were counterstained in Mayer's haematoxylin for 10 seconds, washed in running tap water, and then automatically dehydrated, cleared and mounted.

Electron microscopy

Transmission electron microscopy (TEM) was performed in a paraffin-embedded sample of a perineural mass found in PM-1. The tissue sample was deparaffinized with histoclear, dehydrated with 100% ethanol, infiltrated with LRWhite, sectioned into 60 nm sections and contrasted with uranylacetate. Micrographs were obtained using a FEI Morgagni 268 transmission electron microscope and images were recorded by a side-mounted Olympus Veleta CCD charge-coupled device camera.

RESULTS

Molecular study

Herpesvirus DNA was detected in four (PM-1, PM-4, PM-8, and LM/PM-9) out of the 23 evaluated European minks. Positive HV amplification was observed in 8.5% (12/141) of the analyzed samples, including 11 from postmortem tissue samples and one from an antemortem oral swab (LM/PM-9) (Appendix 2).

Two different glycoprotein B gene sequences were detected in the four HV-positive European mink; one sequence was amplified from PM-1 (mediastinal mass) and PM-8 (lung), and a different one from PM-4 (liver, kidney, brain), and LM/PM-9 (an antemortem oral swab, brain, spinal cord, peripheral nerve [sciatic nerve and brachial plexus], spleen, and bone marrow). The nt and aa identities between both novel glycoprotein B sequences were 79.9% and 86.0%, respectively. The first sequence, found in PM-1 and PM-8, was more similar to the sequence detected in a European badger (MuGHV-1, GenBank Accession number: ABF15169) with, correspondingly, nt and aa identities of 87.2% and 97.8%. The second sequence, found in PM-4 and LM/PM-9, was more related to *Lynx rufus* gammaherpesvirus-2 (ABF15169), with nt identity of 78.4%, and had the highest aa identity (86.0%) with a γ-HV identified in a harp seal (KP136799). A phylogenetic tree based on glycoprotein B amino acid deduced sequences correctly classified the two obtained novel sequences within the cluster of terrestrial mammal γ-HVs, genus *Percavirus*, with bootstrap values above 70% (Figure 1).

A DNA polymerase sequence was amplified in one of the four HV-positive animals (PM-1), while no amplification for that gene was observed in the remaining glycoprotein B gene-positive cases. The highest nt (86.5%) and aa (92.2%) identities of this sequence were to the fisher gammaherpesvirus (HM579931) obtained in another mustelid species, the fisher. The DNA polymerase sequence of PM-1 was submitted to GenBank database under accession number

MN082678, while the glycoprotein B sequences obtained from PM-1 and PM-9 were submitted under accession numbers MN082679 and MN082680, respectively. Since there was a previous report using the terms "Mustelid gammaherpesvirus" (Mustelid gammaherpesvirus-1 or MuGHV-1, Kent et al. [2018]), we have tentatively named the two novel sequences as MuGHV-2 (PM-1 and PM-8) and MuGHV-3 (PM-4 and LM/PM-9). A summary of the γ-HVs detected in mustelids is provided in Table 1.

Retrieval of information prior to death or euthanasia of HV-positive mink

Prior to death, PM-1 presented with corneal opacity in the left eye, protrusion of right eye, severe incoordination, and rear limb weakness, leading to traumatic lesions and inability to eat. PM-4 presented with poor fur quality and compromised vision. PM-8 was uncoordinated and eventually recumbent, which lead to a skin ulcer on its right hip. LM/PM-9 presented with corneal opacity in the left eye and bilateral impaired vision, mild incoordination, rear limbs weakness, and hyporexia that progressed to anorexia. In order to prevent suffering and based on a full clinical examination and complementary examinations (hematology and biochemistry, data not shown), two old animals (over nine years of age; PM-1 and LM/PM-9) were humanely euthanized due to the rapid worsening of clinical signs.

Gross and microscopic findings

The gross and histopathologic findings of the HV-positive mink (PM-1, PM-4, PM-8 and LM/PM-9) are summarized in Appendix 3. The main gross and microscopic findings and suspected cause of death in PM-1 and LM/PM-9 are described below.

PM-1 was a 647-grams male with moderate to severe atrophy of adipose tissue. Protrusion of the right eye due to the presence of a grayish to greenish retrobulbar mass involving the eyelid and peri-ocular skin (Figure 2). The left eye had corneal opacity. Nerves in the left brachial plexus and left elbow joint nerves were surrounded by whitish masses up to 1 cm in greatest dimension (Figure 2). A similar but smaller lesion surrounded the right sciatic nerve distal to the coxofemoral joint. A 5.5x2.8x2.2-cm whitish mass was also found in the caudal mediastinum (Figure 2). The left adrenal gland was partly effaced by a grayish mass 1 cm in diameter (Figure 2).

Microscopically, all masses consisted of a malignant neoplastic proliferation of round cells

characterized by a round, oval, or more rarely irregular, indented or reniform nucleus with 1-2 nucleoli and diverse chromatin patterns, and a low amount of eosinophilic to amphophilic cytoplasm. Anisocytosis, anisokaryosis, and anaplasia were moderate to high, while pleomorphism was moderate. Up to 6 mitoses per 40x power field were observed. Neoplastic cells invaded the perineurium and endoneurium of nerves within the masses (Figures 2 and 3). Affected nerves contained large areas of necrosis with dilatation, vacuolation and fragmentation of myelin sheaths as well as spheroids, deposits of fibrin, infiltrates of neutrophils and lymphocytes, and foci of acute hemorrhage. Neural necrosis extended into the perineural neoplastic tissue, where it was accompanied by prominent infiltration of degenerate neutrophils. Neoplastic cells were present in the perineurium and endoneurium as well. Intralesional within the endoneurium and neoplastic tissue, particularly in areas of necrosis, were syncytia and intranuclear inclusion bodies. These inclusions were predominantly basophilic and filled the nucleus, but eosinophilic inclusions surrounded by a clear halo were noted as well (Figure 3). They were found within syncytia and, presumably, neoplastic cells. Similar infiltrates of neoplastic cells along with fewer well differentiated lymphocytes and plasma cells were present in the spinal cord and root nerves, involving the meninges with a diffuse pattern and neural tissue with a perivascular and multifocal distribution. In the spinal cord, both the white and grey matter was affected (Figure 3). Cerebral meninges were also mildly infiltrated, but predominantly with well differentiated lymphocytes and plasma cells; neoplastic round cells were rare in this location. Neoplastic infiltrates in the retrobulbar mass and adrenal gland caused loss of architecture (Figure 2) and invaded adjacent soft tissues including the skin, adipose tissue and skeletal muscle. Thrombosis was observed in the right eyelid. Other microscopic findings were cataracts in left eye, axonal degeneration in a peripheral skeletal muscle nerve, nodular acinar pancreatic hyperplasia, prostatic hyperplasia, moderate glomerulosclerosis. Additional gross and microscopic findings are summarized in Appendix 3.

PM-9 was a 696-grams male in a good body condition. This mink presented corneal opacity in left eye, and mild thickening of the nictitating membrane. A marked bilateral hemothorax was present, and both lungs were multifocally reddish in color. A mass 0.5 cm diameter was observed in the diaphragmatic lobe of the left lung. This mink had mild to moderate splenomegaly, with a red splenic mass of 0.5 cm in diameter. A cystic mass 1.5 in diameter was also noted in the left liver lobe. A subcutaneous preputial mass measuring 1x0.5x0.3 cm, and mild generalized

lymphadenomegaly were also observed. The adrenal glands contained pale foci less than 1 mm in diameter.

Microscopically, the main disease processes and lesions included pulmonary adenocarcinoma, severe membranous glomerulonephritis, severe chronic diffuse granulomatous lymphadenitis, biliary cystadenoma, and preputial gland cell hyperplasia and cystadenomas with focal malignant transformation and purulent preputial adenitis. Other potential relevant lesions included moderate to marked meningeal mineralization in the lumbar and thoracic spinal cord, mild multifocal spongiosis in the brain, axonal vacuolar degeneration in the thoracic spinal cord and sciatic nerve, as well as nodular hyperplasia of adrenocortical cells, pancreatic acinar and ductal cells and splenic tissue, mild multifocal fibrosis and/or interstitial lymphoplasmacytic nephritis and glomerulosclerosis. Other gross and microscopic findings are summarized in Appendix 3.

Immunohistochemical findings

Positive immunolabeling for the B cell marker CD20 was consistently observed in neoplastic cells in the perineural masses and endoneurium of intra-tumoral nerves (Figure 3). Labeling most notably involved the membrane. No labeling of neoplastic cells was observed for CD3 (Figure 3). Therefore, the lymphoma was classified as a B-cell lymphoma.

Transmission electron microscopy (TEM)

Transmission electron microscopy detected particles approximately 150 nm in diameter in the perineural lymphoma identified in PM-1 (Figure 4). Some of these were similar to empty nucleocapsids while others resembled nucleocapsids containing packaged DNA, and both were compatible with herpesviral particles (Ryner et al., 2006).

DISCUSSION

Two different novel γ-HV sequences were identified in 12 samples from four unrelated adult captive European mink (17.3%, 4/23) that, based on amino acid identities and phylogeny, could be considered novel HV species (MuGHV-2 and MuGHV-3). The prevalence rate should be interpreted with care, once no housekeeping genes were amplified to test the integrity of the DNA present in the samples. This is, to the authors' knowledge, the first report of HV in European mink, expanding the host range of HV infections in mustelids. Other γ-HV species have been previously described in mustelids (King et al., 2004, Tseng et al., 2012, Dalton et al.,

2017), occasionally identified in lesions such as oral ulcerations and plaques (Tseng et al., 2012), and skin ulcers (Gagnon et al., 2011). Nevertheless, this is the first description of γ-HV potentially associated with neoplasms in mustelids.

The two γ-HV-infected European minks with available tissues for histopathology (PM-1 and LM/PM-9) had several neoplasms, including B-cell lymphoma (n=1), pulmonary adenocarcinoma (n=1), biliary cystadenoma (n=1) and preputial cystadenoma (n=1). To the authors' knowledge, these are the first neoplasms described in this species. Age and infectious disease and inbreeding may have played a role in the development of neoplasm. The influence of other factors that may also be implicated, such as environmental contamination or inbreeding, was not assessed. In other carnivore species, for instance the California sea lion (*Zalophus californianus*), collaborative studies showed that certain neoplasms (urogenital carcinoma) were associated with genotype, but also with HV and persistent organic pollutants (King et al., 2002; Browning et al., 2015).

In regard to age, both animals with neoplasms and HV-infection (PM-1 and LM/PM-9) were considered to be of advanced age for the species (over nine years old). The oldest recorded free-ranging European mink was five years old; however, captive animals can reach ten years of age (Mañas et al., 2016a). The nodular acinar pancreatic hyperplasia, prostatic hyperplasia and glomerulosclerosis observed in PM-1, as well as nodular acinar and ductal pancreatic hyperplasia, and nodular splenic hyperplasia in LM/PM-9 were possibly related to aging. Aging should be considered an immunosuppression factor per se (Marchioni & Berzero, 2015), capable of facilitating neoplasm development.

The European mink with neoplasms - PM-1 and LM/PM-9 – were infected with gammaherpesviruses MuGHV-2 and MuGHV-3, respectively. HV-compatible particles were observed by TEM in a B-cell lymphoma with neural tissue tropism of PM-1, in which intratumoral syncytia and intranuclear inclusion bodies characteristic of herpesviruses were noted. Noteworthy, viruses have been associated with approximately 15% to 20% of human cancers worldwide (Parkin et al., 2006; Boccardo & Villa, 2007). Several γ-HV are oncogenic viruses. For instance, Epstein–Barr virus (*Human gammaherpesvirus 4*) has been etiologically associated with a broad range of lymphoproliferative lesions and B-, T- and NK-cell malignant lymphomas in humans (Shannon-Lowe et al., 2017), including B-cell lymphoma in elderly

populations, possibly associated with immunosuppression due to aging (El Jamal, 2014; Castillo et al., 2016). Kaposi sarcoma-associated HV (syn. *Human gammaherpesvirus 8*) is associated with Kaposi's sarcoma and lymphoproliferative disorders in humans (Du et al., 2007). In wild mammals, γ-HVs have been implicated in the pathogenesis of several neoplastic diseases, including urogenital carcinoma or multicentric B-cell lymphoblastic lymphoma in California sea lion (Lipscomb et al., 2000; Venn-Watson et al., 2012; Browning et al., 2015). Gammaherpesvirus-associated lymphoproliferative disease has been observed in captive non-human primates of the family Callitrichidae (Ramer et al., 2000). The experimental inoculation of γ-HV saimiri herpesvirus in three-striped night monkeys (*Aotus trivirgatus*) induced acute lymphocytic leukemia (Melendez et al., 1971), while Epstein-Barr virus inoculation caused lymphoma in cotton-top tamarins (*Saguinus oedipus*) (Miller et al., 1977). The herpesviruses identified in both mink, particularly in PM-1, may have been involved in the etiopathogenesis of the neoplasms found. Conversely, the detection of γ-HVs in several tissues from infected animals presenting neoplasms could have been caused by viral reactivation from latency, triggered by, among other causes, immunosuppression (which could be associated with the presence of neoplasms), given that γ-HVs become latent in lymphoid cells (Roizmann et al., 1992).

In the domestic ferret, a species closely related to the European mink, lymphomas are common spontaneous malignancies. Healthy ferrets experimentally inoculated with non-cellular extracts from ferrets with lymphoma also developed this neoplasm, which reinforces the potential role of infectious agents in the horizontal transmission of lymphomas in this species (Erdman et al., 1995). The role of *Aleutian mink disease virus* and retrovirus infection has been suggested (Erdman et al., 1992). Unfortunately, due to economic constraints, the potential role of retroviruses in European minks has not been assessed yet.

Inbreeding is another factor that could partially explain the observed neoplasms. The French and Spanish European minks appear to be highly inbred (Maran et al., 2016), and it would be interesting to know if these highly genetically uniform populations are more prone to neoplasia. For instance, the loss or lack of major histocompatibility complex (MHC) diversity, known to reduce immune response effectiveness, is postulated to contribute to the successful spread of the devil facial tumour disease of Tasmanian devils (*Sarcophilus harrisii*) (Siddle et al., 2007). The association between neoplasm (urogenital carcinoma) and inbreeding has also been identified in California sea lion (Acevedo-Whitehouse et al., 2003).

The neurological clinical signs – mainly incoordination and rear limb weakness, presented by three of the four HV-positive animals (PM-1, PM-8, LM/PM-9, all over 9 years of age) were initially considered typical signs of weakness or aging-related degenerative disorders. The microscopic lesions described in the peripheral and central nervous systems of two of the examined animals potentially explain the observed neurological signs: peripheral and central nervous system B-cell lymphomas, axonal degeneration, and peripheral skeletal muscle nerves axonal degeneration (PM-1), and brain spongiosis, and spinal cord and sciatic nerve axonal vacuolar degeneration (LM/PM-9). The spongiosis and axonal degeneration observed in LM/PM-9 could be associated with metabolic (e.g., renal encephalopathy) and/or toxic disorders. Noteworthy, LM/PM-9 had severe glomerulonephritis, mild interstitial lymphoplasmacytic nephritis, glomerulosclerosis and azotemia, with high urea (410 mg/dl) and creatinine levels (1.44 mg/dl). These were elevated when compared with the reference values described in other mustelid, the ferret: 11-42 mg/dl and 0.2-1 mg/dl, respectively (Carpenter & Marion, 2017) and the remaining European minks analyzed in this study (data not shown), which could explain the incoordination signs. No reference values are available for European mink.

Interestingly, the MuGHV-2 found in case PM-1 presented neural tissue tropism, with HV particles observed in a perineural mass, and similarly, LM/PM-9 samples of brain, spinal cord, peripheral nerve (sciatic nerve and brachial plexus) were positive to MuGHV-3. Both animals had incoordination. The etiology of the neuritis in the B-cell lymphoma of PM-1 is unclear; it could have been due to secondary inflammation associated with the local necrosis or a direct response against herpesviral infection. Some γ-HVs have marked neurotropism, such as *Human herpesvirus 4*/ Epstein–Barr virus and *Human herpesvirus 4*/Kaposi's sarcoma-associated HV (KSHV) (El Jamal et al., 2014; Tso et al., 2016). For instance, Epstein–Barr virus has been suggested to cause CNS damage by parainfectious and direct virus-related mechanisms in humans (e.g., meningitis, encephalitis and lymphoma) (El Jamal et al., 2014). Thus, it is not possible to exclude HVs as the potential causative agents of the nervous clinical signs observed in these infected mink. Cataracts, corneal melanosis, focal granulomatous conjunctivitis in left eye, and protrusion of and periocular mass around the right eye observed in PM-1 may have contributed to its impaired vision. All mink were seronegative to two other viral agents that could also cause neurological clinical signs and/or impaired vision: *Aleutian mink disease virus* (Hadlow, 1982; Dyer et al., 2000), and canine distemper (Summers et al., 1984). Histopathologic

evidence of infection with *Toxoplasma gondii*, *Encephalitozoon* spp. or *Sarcocystis neurona* was not observed.

One of the novel European mink γ-HVs (Mu-GHV3) was detected in an antemortem oral swab (LM-9), suggesting that viral shedding occurs in infected European minks and, therefore, that horizontal HV transmission through oral secretions could be possible. Such characteristic has been previously identified in γ-HV viruses; Epstein–Barr virus is commonly transmitted via saliva (Marchioni & Berzero, 2015), and other γ-HVs have been detected in sea otter oral mucosal ulcers and plaques (Tseng 2012), and in oral tissue and swabs samples from northern elephant seals (*Mirounga angustirostris*) (Goldstein et al., 2006). None of the mink in this study has oral ulcers. Transmission can be enhanced in captivity as close confinement leads to a higher contact rate between animals and stress-related immunosuppression (Tseng et al., 2012). Interestingly, one of the infected European minks (LM/PM-9) had lesions compatible with chronic stress (bilateral nodular hyperplasia of adrenocortical cells), which could reactivate latent γ-HV in the lymphoid tissue (Roizmann et al., 1992; Lam et al., 2013).

Three of the HV-infected European minks were captured in the Ebro River basin (PM-4, PM-8 and LM/PM-9). The fourth one (PM-1) was born in Pont de Suert in 2006. Herpesvirus can cause lifelong infections (Roizmann et al., 1992); therefore, it was not possible to establish if these animals became infected during their stay in the captive breeding center (the virus was detected when they had already been in captivity for several years) or already carried the virus when they joined the collection. As several European mink conservation programs involving species restoration and reintroduction use animals bred in captivity (Mañas et al., 2001), future studies should investigate whether these HVs are present in wild European mink populations. Due to the fact that several HV infections predispose the host to secondary bacterial infections (Cabello et al., 2013), and considering the small size of the European mink population, the authors believe that monitoring for these viruses should be considered when implementing conservation strategies including translocations, as has been advised for other species, e.g., the Darwin's fox (*Lycalopex fulvipes*) (Cabello et al., 2013).

CONCLUSIONS

This is the first report of HV in European minks. Four European minks were positive to one of the two identified novel herpesviruses: *Mustelid gammaherpesvirus 2* (MuGHV-2) and *Mustelid*

gammaherpesvirus 3 (MuGHV-3). Several neoplasms, including B-cell lymphoma, adenocarcinoma and biliary and preputial cystadenoma, as well as neurological signs, were observed in some of the γ-HV-infected European minks. Aside from the B-cell lymphoma case potentially associated with MuGHV-2, the relationship between γ-HV infection and the remaining lesions is unclear.

This study contributes to the conservation of European minks by expanding the current knowledge on the viral diseases affecting this species. Additional research is needed to establish the prevalence of these novel γ-HVs in free-ranging European mink populations, and to investigate their pathogenicity and the role of herpesvirus and other potential cofactors in the neoplasms detected in this particular European mink captive breeding population. This information will be critical to take more scientifically based decisions and adopt management techniques for the conservation of this endangered species, as well as to determine if infected captive bred European minks could be released into the wild without negatively impacting the species' conservation.

Acknowledgements

We thank the Pont de Suert Captive Breeding Center staff for their assistance and for providing data and audiovisual information on the studied animals and Lene C. Hermansen (Imaging Center, Norwegian University of Life Sciences) for the TEM analysis. We also thank Francesc Mañas (Department of Environment, Generalitat de Catalunya) and Madis Podra (European Mink Association) for their support and interest in this project, and for providing the information regarding the studied animals, and Francisco Fernandez Rivera, Head of the Environmental management in Forestal Catalana, for authorizing this study. Ana Carolina Ewbank receives a doctoral-fellowship from the São Paulo Research Foundation (FAPESP, process number 2018/20956-0). Carlos Sacristán is a recipient of a post-doctoral fellowship by the FAPESP (process number 2018/25069-7). This study was funded by the Innovation Initiative Grant (IIG) and by donors of the Edinburgh Fund (University of Edinburgh).

Conflict of Interest Statement: the authors declare no conflict of interest.

Data Availability Statement: The data that supports our findings are available in the manuscript and in the supplementary material.

REFERENCES

Acevedo-Whitehouse, K., Gulland, F., Greig, D., & Amos, W. (2003). Inbreeding: disease susceptibility in California sea lions. *Nature*, *422*, 35. https://doi.org/10.1038/422035a

Banks, M., King, D. P., & Daniells, C. (2002). Partial characterization of a novel gammaherpesvirus isolated from a European badger (*Meles meles*). *Journal of General Virology*, *83*, 1325–1330. https://doi.org/ 10.1099/0022-1317-83-6-1325

Bodewes, R., Ruiz-Gonzalez, A., Schapendonk, C. M., van den Brand, J. M., Osterhaus, A.D., & Smits, S. L. (2014). Viral metagenomic analysis of feces of wild small carnívores. *Virology Journal*, *11*, 89. https://doi.org/ 10.1186/1743-422X-11-89

Boccardo, E., & Villa, L. L. (2007). Viral origins of human cancer. *Current Medicinal Chemistry*, *14*, 2526–2539. doi: https://doi.org/10.2174/092986707782023316

Browning, H. M., Gulland, F. M. D., & Hammond, J. A. (2015). Common cancer in a wild animal: the California sea lion (*Zalophus californianus*) as an emerging model for carcinogenesis. *Philosophical Transactions of the Royal Society B*, *370*, 1673. https://doi.org/10.1098/rstb.2014.0228.

Cabello, J., Esperón, F., Napolitano, C., Hidalgo, E., Dávila, J. A., & Millán, J. (2013). Molecular identification of a novel gammaherpesvirus in the endangered Darwin's fox (*Lycalopex fulvipes*). *Journal of General Virology*, *94*, 2745–2749. https://doi.org/10.1099/vir.0.057851-0.

Carpenter, J. W., & Marion, C. (2017). *Exotic Animal Formulary* (5th ed.). Philadelphia, PA: Saunders.

Castillo, J. J., Beltran, B. E., Miranda, R. N., Young, K. H., Chavez, J. C., & Sotomayor, E. M. (2016). EBV-positive diffuse large B-cell lymphoma of the elderly: 2016 update on diagnosis, risk-stratification, and management. *American Journal of Hematology*, *91*, 529-537. https://doi.org/10.1002/ajh.24370

Dalton, C. S., van de Rakt, K., Fahlman, Å., Ruckstuhl, K., Neuhaus, P., Popko, R., Kutz, S., & van der Meer, F. (2017). Discovery of herpesviruses in Canadian wildlife. *Archives of Virology*, *162*, 449-456

Dandár, E., Szabó, L., & Heltai, M. (2010). PCR screening of mammalian predators (Carnivora) for adenoviruses and herpesviruses: the first detection of a mustelid herpesvirus in Hungary. *Magyar Allatorvosok Lapja*, *132*, 302-308.

Du, M. -Q., Bacon, C. M., & Isaacson, P. G. (2007). Kaposi sarcoma-associated herpesvirus/human herpesvirus 8 and lymphoproliferative disorders. *Journal of Clinical Pathology*, *60*, 1350-1357.

Dyer, N. W., Ching, B., & Bloom, M. E. (2000). Nonsuppurative meningoencephalitis associated with Aleutian mink disease parvovirus infection in ranch mink. *Journal of Veterinary Diagnostic Investigation*, *12*, 159–162. https://doi.org/10.1177/104063870001200212

Ehlers, B., Dural, G., Yasmum, N., Lembo, T., de Thoisy, B., Ryser-Degiorgis, M. P., Ulrich, R. G., & McGeoch, D. J. (2008). Novel mammalian herpesviruses and lineages within the Gammaherpesvirinae: cospeciation and interspecies transfer. *Journal of Virology*, *82*, 3509–3516. https://doi.org/10.1128/JVI.02646-07.

El Jamal, S., Li, S., Bajaj, R., Wang, Z., Kenyon, L., Glass, J., Pang, C.S., Bhagavathi, S., Peiper, S. C., & Gong, J. Z. (2014). Primary central nervous system Epstein–Barr virus-positive diffuse large B-cell lymphoma of the elderly: a clinicopathologic study of five cases. *Brain Tumor Pathology*, *31*, 265–273. https://doi.org/10.1007/s10014-013-0173-x

Erdman, S. E., Moore, F. M., Rose, F. M., & Fox, J. G. (1992). Malignant lymphoma in ferrets: clinical and pathological findings in 19 cases. *Journal of Comparative Pathology*, *106*, 37–47. https://doi.org/10.1016/0021-9975(92)90066-4

Erdman, S. E., Reimann, K. A., Moore, F. M., Kanki, P. J., Yu, Q. C., & Fox, J. G. (1995). Transmission of a chronic lymphoproliferative syndrome in ferrets. *Laboratory Investigation; a Journal of Technical Methods and Pathology*, *72*, 539-546.

Ferrer, M. (2014). Life Lutreola Spain (2014-2018). Retrieved from http://ec.europa.eu/environment/life/project/Projects/index.cfm?fuseaction=search.dspPage&n_proj_id=4908

Fournier-Chambrillon, C., Aasted, B., Perrot, A., Pontier, D., Sauvage, F., Artois, M., Cassiède, J. M., Chauby, X., Dal Molin, A., Simon, C., & Fournier, P. (2004). Antibodies to Aleutian mink disease parvovirus in free-ranging European mink (*Mustela lutreola*) and other small carnivores

from southwestern France. *Journal of Wildlife Diseases*, *40*, 394-402. https://doi.org/10.7589/0090-3558-40.3.394

Gagnon, C. A., Tremblay, J., Larochelle, D., Music, N., & Tremblay, D. (2011). Identification of a novel herpesvirus associated with cutaneous ulcers in a fisher (*Martes pennanti*). *Journal of Veterinary Diagnostic Investigation*, *23*, 986–990. https://doi.org/10.1177/1040638711418615.

Goldstein, T., Lowenstine, L. J., Lipscomb, T. P., Mazet, J. A., Novak, J., Stott, J. L., & Gulland, F. M., (2006). Infection with a novel gammaherpesvirus in northern elephant seals (*Mirounga angustirostris*). *Journal of Wildlife Diseases*, *42*, 830–835. https://doi.org/10.7589/0090-3558-42.4.830

Goldstein, T., Gill, V. A., Tuomi, P., Monson, D., Burdin, A., Conrad, P. A., Dunn, J. L., Field, C., Johnson, C., Jessup, D. A., Bodkin, J., & Doroff, A. M. (2011). Assessment of clinical pathology and pathogen exposure in sea otters (*Enhydra lutris*) bordering the threatened population in Alaska. *Journal of Wildlife Diseases*, *47*, 579-592. https://doi.org/10.7589/0090-3558-47.3.579

Gorham, J. R., Hartsough, G. R., & Burger, D. (1998). An epizootic of pseudorabies in ranch mink. *Scientifur*, *22*, 243-245.

Guzmán, D. S. M., Carvajal, A., García-Marín, J. F., Ferreras, M. C., Pérez, V., Mitchell, M., Urra, F., & Ceña, J. C. (2008). Aleutian disease serology, protein electrophoresis, and pathology of the European mink (*Mustela lutreola*) from Navarra, Spain. *Journal of Zoo and Wildlife Medicine*, *39*, 305–313. https://doi.org/10.1638/2006-0033.1

Hadlow, W. J. (1982). Ocular lesions in mink affected with Aleutian disease. *Veterinary Pathology*, *19*, 5–15. https://doi.org/10.1177/030098588201900103

Huff, J. L., & Barry, P. A. (2003). B-Virus (*Cercopithecine herpesvirus*1) infection in humans and macaques: potential for zoonotic disease. *Emerging Infectious Diseases*, *9*, 246-250. https://doi.org/10.3201/eid0902.020272

ICTV (International Committee on Taxonomy of Viruses). (2017). Virus Taxonomy: The Classification and Nomenclature of Viruses. Online (9th) Report of the ICTV. Email ratification 2017 (MSL #31). Retrieved from https://talk.ictvonline.org/ictv-reports/ictv_online_report/

Kent, A., Ehlers, B., Mendum, T., Newman, C., Macdonald, D. W., Chambers, M., & Buesching, C. D. (2018). Genital tract screening finds widespread infection with Mustelid Gammaherpesvirus 1 in the European badger (*Meles meles*). *Journal of Wildlife Diseases*, *54*, 133-137. https://doi.org/10.7589/2016-12-274

King, D. P., Hure, M. C., Goldstein, T., Aldridge, B. M., Gulland, F. M., Saliki, J. T., Buckles, E. L., Lowenstine, L. J., & Stott, J. L. (2002). Otarine herpesvirus-1: a novel gammaherpesvirus associated with urogenital carcinoma in California sea lions (*Zalophus californianus*). *Veterinary Microbiology*, *86*, 131-137. https://doi.org/10.1016/s0378-1135(01)00497-7

King, D. R., Mutukwa, N., Lesellier, S., Cheeseman, C., Chambers, M. A., & Banks, M. (2004). Detection of Mustelid herpesvirus-1 infected European badgers (*Meles meles*) in the British Isles. *Journal of Wildlife Diseases*, *40*, 99–102. https://doi.org/10.7589/0090-3558-40.1.99

Kumar, S., Stecher, G., Tamura, K. (2016). MEGA7: Molecular Evolutionary Genetics Analysis version 7.0 for bigger datasets. *Molecular Biology and Evolution*, *33*, 1870–1874. https://doi.org/10.1093/molbev/msw054

Lam, L., Garner, M. M., Miller, C. L. (2013). A novel gammaherpesvirus found in oral squamous cell carcinomas in sun bears (*Helarctos malayanus*). Journal *of Veterinary Diagnostic Investigation*, *25*, 99–106.

Lipscomb, T. P., Scott, D. P., Garber, R. L., Krafft, A. E., Tsai, M. M., Lichy, J. H., Taubenberger, J. K., Schulman, F. Y., & Gulland, F. M. (2000). Common metastatic carcinoma of California sea lions (*Zalophus californianus*): evidence of genital origin and association with novel gammaherpesvirus. *Veterinary Pathology*, *37*, 609–617. https://doi.org/10.1354/vp.37-6-609

Liu, H., Li, X. T., Hu, B., Deng, X. Y., Zhang, L., Lian, S. Z., Zhang, H. L., Lv, S., Xue, X. H., Lu, R. G., Shi, N., Yan, M. H., Xiao, P. P., & Yan, X. J. (2017). Outbreak of severe pseudorabies virus infection in pig-offal-fed farmed mink in Liaoning Province, China. *Archives of Virology*, *162*, 863-866. https://doi.org/10.1007/s00705-016-3170-7.

Lodé, T., Cormier, J. P., & Le Jacques, D. (2001). Decline in endangered species as an indication of anthropic pressures: the case of European mink *Mustela lutreola* Western population. *Environmental Management*, 28, 727-735. https://doi.org/10.1007/s002670010257

Mañas, S., Ceña, J. C., Ruiz-Olmo, J., Palazón, S., Domingo, M., Wolfinbarger, J. B., & Bloom, M. E. (2001). Aleutian mink disease parvovirus in wild riparian carnivores in Spain. *Journal of Wildlife Diseases*, *37*, 138-144. https://doi.org/10.7589/0090-3558-37.1.138

Mañas, S., Gómez, A., Asensio, V., Palazón, S., Pŏdra, M., Casal, J., & Ruiz-Olmo, J. (2016a). Demographic structure of three riparian mustelid species in Spain. *European Journal of Wildlife Research*, *62*, 119-129. https://doi.org/10.1007/s10344-015-0982-9

Mañas, F., Gómez, A., Asensio, V., Palazón, S., Podra, M., Alarcia, O.E., Ruiz-Olmo, J., & Casa, J. (2016b). Prevalence of antibody to aleutian mink disease virus in European mink (*Mustela lutreola*) and american mink (*Neovison vison*) in Spain. *Journal of Wildlife Diseases*, *52*, 22–32. https://doi.org/10.7589/2015-04-082

Maran, T., Skumatov, D., Gomez, A., Põdra, M., Abramov, A. V., & Dinets, V. (2016). *Mustela lutreola*. The IUCN Red List of Threatened Species 2016. Retrieved from https://www.iucnredlist.org/species/14018/45199861

Marchioni, E., & Berzero, G. (2015). Viral Infections of the Nervous System, In A. Sghirlanzoni, G. Lauria, L. Chiapparini (Eds.), *Prognosis of Neurological Diseases*. (pp. 75-92) Milan, Italy: Springer-Verlag Italia. https://doi.org/10.1007/978-88-470-5755-5

Melendez, L. V., Hunt, R. D., Daniel, M. D., Blake, B. J., & Garcia, F. G. (1971). Acute lymphocytic leukemia in owl monkeys inoculated with herpesvirus saimiri. *Science*, *171*, 1161–1163. https://doi.org/10.1126/science.171.3976.1161

Miller, G., Shope, T., Coope, D., Waters, L., Pagano, J., Bornkamn, G., & Henle, W. (1977). Lymphoma in cotton-top marmosets after inoculation with Epstein-Barr virus: tumor incidence, histologic spectrum antibody responses, demonstration of viral DNA, and characterization of viruses. *Journal of Experimental Medicine, 145*, 948–967. https://doi.org/10.1084/jem.145.4.948

Parkin, D. M. (2006). The global health burden of infection-associated cancers in the year 2002. *International Journal of Cancer*, *118*, 3030–3044. https://doi.org/10.1002/ijc.21731

Philippa, J., Fournier-Chambrillon, C., Fournier, P., Schaftenaar, W., van de Bildt, M., van Herweijnen, R., Kuiken, T., Liabeuf, M., Ditcharry, S., Joubert, L., Bégnier, M., & Osterhaus, A. (2008). Serologic survey for selected viral pathogens in free-ranging endangered European mink (*Mustela lutreola*) and other mustelids from south-western France. *Journal of Wildlife Diseases*, *44*, 791–801. https://doi.org/10.7589/0090-3558-44.4.791

Quiroga, M. I., López-Peña, M., Vázquez, S., & Nieto, J. M. (1997). Distribution of Aujeszky's disease virus in experimentally infected mink (*Mustela vison*). *Deutsche tierärztliche Wochenschrift*, *104*, 147-150.

Ramer, J. C., Garber, R. L., Steele, K. E., Boyson, J. F., O'Rourke, C., & Thomson, J. A. (2000). Fatal lymphoproliferative disease associated with a novel gammaherpesvirus in a captive population of common marmosets. *Comparative Medicine*, *50*, 59-68.

Reading, M. J., & Field, H. J. (1999). Detection of high levels of canine herpes virus 1 neutralising antibody in kennel dogs using a novel serum neutralisation test. *Research in Veterinary Science*, *66*, 273-275. https://doi.org/10.1053/rvsc.1998.0222

Reimer, D. C., & Lipscomb, T. P. (1998). Malignant seminoma with metastasis and herpesvirus infection in a free-living sea otter (*Enhydra lutris*). *Journal of Zoo and Wildlife Medicine*, *29*, 35-39.

Roizmann, B., Desrosiers, R. C., Fleckenstein, B., Lopez, C., Minson, A. C., & Studdert, M. J. (1992). The family *Herpesviridae*: an update. *Archives of Virology*, *123*, 425–449. https://doi.org/10.1007/bf01317276

Ryner, M., Strömberg, J. O., Söderberg-Nauclér, C., & Homman-Loudiyi, M. (2006). Identification and classification of human cytomegalovirus capsids in textured electron micrographs using deformed template matching. *Virology Journal*, *3*, 57. https://doi.org/10.1186/1743-422X-3-57

Shannon-Lowe, C., Rickinson, A. B., & Bell, A. I. (2017). Epstein–Barr virus-associated lymphomas. *Philosophical Transactions of the Royal Society B*, *372*, 20160271. https://doi.org/10.1098/rstb.2016.0271

Siddle, H. V., Kreiss, A., Eldridge, M. D., Noonan, E., Clarke, C. J., Pyecroft, S., Woods, G. M., & Belov, K. (2007). Transmission of a fatal clonal tumor by biting occurs due to depleted MHC diversity in a threatened carnivorous marsupial. *Proceedings of the National Academy of Sciences of the United States of America*, *104*, 16221–16226. https://doi.org/10.1073/pnas.0704580104

Sin, Y. W., Annavi, G., Dugdale, H. L., Newman, C., Burke, T., & MacDonald, D. W. (2014). Pathogen burden, co-infection and major histocompatibility complex variability in the European badger (*Meles meles*). *Molecular Ecology*, *23*, 5072–5088. https://doi.org/10.1111/mec.12917.

Summers, B., Greisen, H., & Appel, M. J. (1984). Canine distemper encephalomyelitis: variation with virus strain. *Journal of Comparative Pathology*, *94*, 65-75. https://doi.org/10.1016/0021-9975(84)90009-4

Tseng, M., Fleetwood, M., Reed, A., Gill, V. A., Harris, R. K., Moeller, R. B., Lipscomb, T. P., Mazet, J. A., & Goldstein, T. (2012). Mustelid Herpesvirus-2, a novel herpes infection in northern sea otters (*Enhydra lutris kenyoni*). *Journal of Wildlife Diseases*, *48*, 181–185. https://doi.org/10.7589/0090-3558-48.1.181

Tso, F. Y., Sawyer, A., Kwon, E. H., Mudenda, V., Langford, D., Zhou, Y., West, J., & Wood, C. (2016). Kaposi's Sarcoma–Associated Herpesvirus Infection of Neurons in HIV-Positive Patients. *The Journal of Infectious Diseases*, *215*, 1898-1907. https://doi.org/10.1093/infdis/jiw545.

VanDevanter, D. R., Warrener, P., Bennett, L., Schultz, E. R., Coulter, S., Garber, R. L., & Rose, T. M. (1996). Detection and analysis of diverse herpesviral species by consensus primer PCR. *Journal of Clinical Microbiology*, *34*, 1666–1671.

Venn-Watson, S., Benham, C., Gulland, F. M., Smith, C. R., St Leger, J., Yochem, P., Nollens, H., Blas-Machado, U., Saliki, J., Colegrove, K., Wellehan, J. F. Jr., & Rivera, R. (2012). Clinical relevance of novel Otarine herpesvirus-3 in California sea lions (*Zalophus californianus*): Lymphoma, esophageal ulcers, and strandings. *Veterinary Research*, *43*, 85. https://doi.org/10.1186/1297-9716-43-85

Wang, G., Du, Y., Wu, J. Q., Tian, F. L., Yu, X. J., & Wang, J. B. (2018). Vaccine resistant pseudorabies virus causes mink infection in China. *BMC Veterinary Research*, *14*, 20. https://doi.org/10.1186/s12917-018-1334-2

Widén, F., Das Neves, C. G., Ruiz-Fons, F., Reid, H. W., Kuiken, T., Gavier-Widén, D., & Kaleta, E. F. (2012). *Herpesvirus Infections*. In D. Gavier-Widén, P. J. Duff, & A. Meredith. (Eds.), *Infectious Diseases of Wild Mammals and Birds in Europe*. (pp. 3–36). Ames: Blackwell Publishing Ltd. https://doi.org/10.1002/9781118342442

637 **Table 1.** Herpesviruses infections described in the family Mustelidae.

Species	HV name in the article	GenBank access nº.	Lesions attributable to herpesvirus	PCR prevalence	Tissue	Country	Author
European badger (*Meles meles*)	Mustelid herpesvirus 1 (MusHV-1, γ-HV)	AF376034 AY050215 AF275656	Cytopathic effect on badger' pulmonary fibroblasts	Single case	Pulmonary fibroblasts	UK	Banks et al. (2002)
	Mustelid herpesvirus-1 (MusHV-1, γ-HV)	Not provided	Not described	95% (18/19) 100% (10/10)	Blood Blood	UK Ireland	King et al. (2004)
	Mustelid herpesvirus-1 (MusHV-1, γ-HV)	GU799569	Not reported (detected in a road-kill animal)	Single case		Hungary	Dandár et al. (2010)
	Mustelid herpesvirus-1 (MusHV-1, γ-HV)	Not provided	Not described	98.1% (354/361)	Blood	UK	Sin et al. (2014)
	Mustelid gammaherpesvirus 1	AF275657	Not described	Single case	Lung	Not described	Unpublished
	Mustelid alphaherpesvirus 1	MF042164	Not described	Single case	Mediastinal lymph node	France	Unpublished
	Mustelid gammaherpesvirus-1 (MusGHV-1)	Not provided	Not detected	55% (54/98)	Genital swabs	UK	Kent et al. (2018)
Northern sea otter (*Enhydra lutris kenyoni*)	Mustelid herpesvirus-2 (MusHV-2, γ-HV)	GU979535	Presence of ulcers or pale raised plaques on the lingual, gingival, oral, esophageal and labial mucosa: epithelial hyperplasia and hyperkeratosis, often with epithelial cell degeneration and ulceration, and presence of eosinophilic intranuclear inclusion	46% (13/28)	Skin biopsies	United States	Tseng et al. (2012)

			bodies) Apparently healthy animal	34% (21/62)	nasal swabs	United States	
Oriental small-clawed otter (*Aonyx cinerea*)	Oriental small-clawed otter gammaherpesvirus (γ-HV)	FJ797657	Not described	Single case	Not described	Hungary	Unpublished
Captive fisher (*Martes pennanti*)	Fisher herpesvirus (FiHV, γ-HV)	HM579931	Multiple skin ulcers on the muzzle and plantar pads (thickened epidermis with increased numbers of koilocytes, perinuclear vacuolation, nuclear hypertrophy, pale amphophilic intranuclear inclusion bodies, and basophilic pseudoinclusions)	Single case	Skin ulcers	Born in captivity in the Unites States and sent to Canada	Gagnon et al. (2011)
American marten (*Martes americana*)	Marten alphaherpesvirus	KX062131 KX062132 KX062133	Not described	3 cases	Not described	Canada	Dalton et al. (2017)
	Marten betaherpesvirus	KX062129 KX062134 KX062135 KX062136	Not described	4 cases	Not described		
	Marten gammaherpesvirus 1	KX062128	Not described	2 cases	Not described		
	Marten gammaherpesvirus 2	KX062130					
European mink (*Mustela lutreola*)	Mustelid gammaherpesvirus-2	MN082678, MN082679	Basophilic (or eosinophilic, rarely found) inclusion bodies, and syncytia in a multifocal neural and perineural lymphoma.	8.7% (2/23)	Mediastinal B-cell lymphoma and lung	Spain	This work

	Mustelid gammaherpesvirus-3	MN082680	Not detected	8.7% (2/23)	Oral swab, kidney, liver, spleen, bone marrow, brain, spinal cord, sciatic nerve and brachial plexus

638

FIGURES

Figure 1. Maximum likelihood phylogram of the alignment of the obtained deduced amino acid gammaherpesvirus sequences (marked with red dots) and other herpesvirus sequences retrieved from GenBank. *Ictalurid herpesvirus 1* was selected as outgroup. The reliability of the tree was tested by bootstrap analysis with 1,000 replicates, and those bootstrap values lower than 70 were omitted.

Figure 2. Gross and microscopic findings in European mink (*Mustela lutreola*) PM-1: **(A)** Periocular mass (white arrow). Scale bar = 1 centimeter. **(B)** Retrobulbar mass (right eye, black arrow). Scale bar = 1 centimeter. **(C)** Perineural mass along the brachial plexus (black arrows) and mediastinal mass (white arrow). Scale bar = 1 centimeter. **(D)** Mass effacing the left adrenal gland (black arrow). **(E)** Note diffuse infiltration of neoplastic lymphocytes in the perineural tissues and endoneurium of the brachial plexus mass; n = nerves (hematoxylin and eosin). **(F)** Adrenal gland (a) is invaded by lymphoma (delimited with arrowheads) (hematoxylin and eosin).

Figure 3. Microscopic and immunohistochemical findings in European mink (*Mustela lutreola*) PM-1: **(A)** Higher magnification of endoneural (arrows) and perineural lymphoid infiltrates in the brachial plexus mass. Note necrosis of neural tissue (asterisk). **(B)** A higher magnification of neoplastic infiltrates demonstrates neoplastic lymphoblasts (hematoxylin and eosin). **(C)** Note numerous basophilic intranuclear inclusion bodies (red arrowheads) in unidentified cells and syncytia (black arrows) and few eosinophilic intranuclear inclusion bodies surrounded by a clear halo (black arrowhead) in an area of necrosis involving a nerve in the brachial plexus with perineural and neural lymphoma (hematoxylin and eosin). **(D)** Lymphoma involving the spinal cord, particularly the pachymeninges (delimited with black arrowheads) but also the white and grey matter (red arrowheads) (hematoxylin and eosin). **(E)** Note positive immunolabeling for CD20 in perineural and endoneural neoplastic lymphocytes in the brachial plexus mass. **(F)** Neoplastic lymphocytes are not labeled with CD3 antibodies.

Figure 4. Transmission electron microscopy (TEM) of the perineural lymphoma found in European mink (*Mustela lutreola*) PM-1: **(A)** Intracytoplasmic herpesvirus-like particle (red

arrow) after nuclear egression but prior to acquiring the secondary envelopment in the cytoplasm (which leads to the well-known enveloped herpesvirus particles seen on mature virions) and nuclear membrane (yellow arrow), **(B)** Detailed view of the same particle (red arrow) and nuclear membrane (yellow arrow).

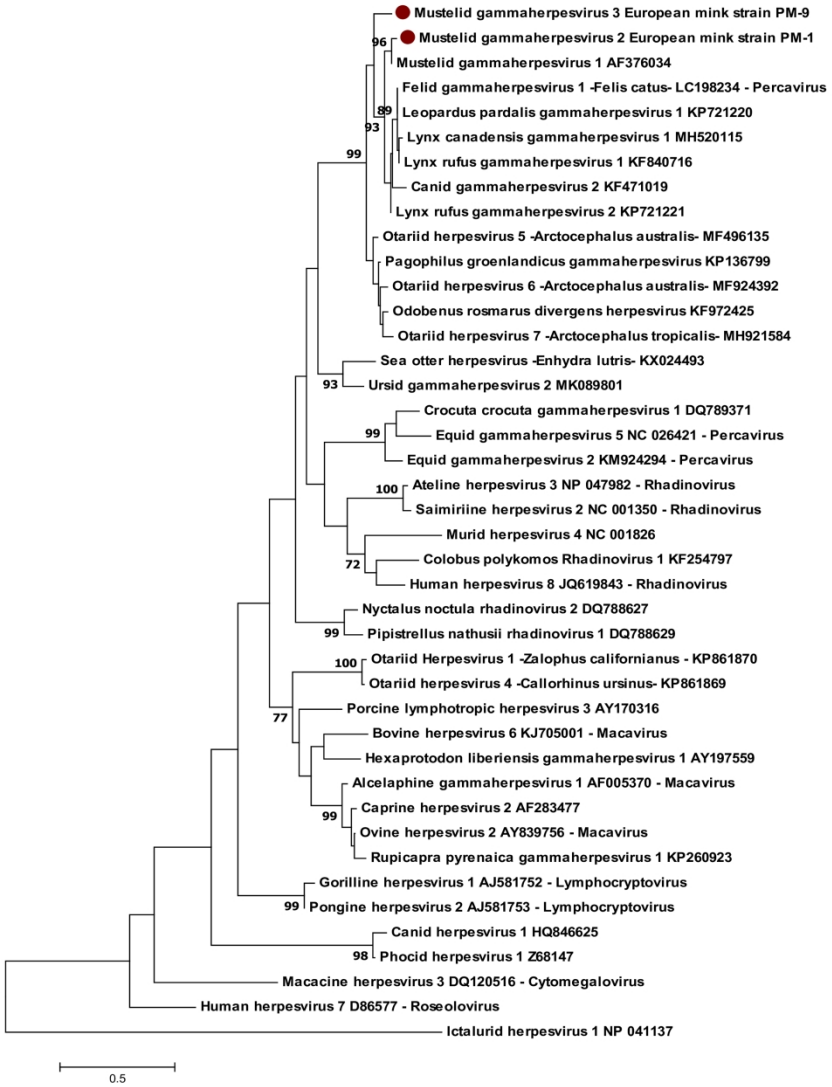

Figure 1. Maximum likelihood phylogram of the alignment of the obtained deduced amino acid gammaherpesvirus sequences (marked with red dots) and other herpesvirus sequences retrieved from GenBank. Ictalurid herpesvirus 1 was selected as outgroup. The reliability of the tree was tested by bootstrap analysis with 1,000 replicates, and those bootstrap values lower than 70 were omitted.

180x254mm (600 x 600 DPI)

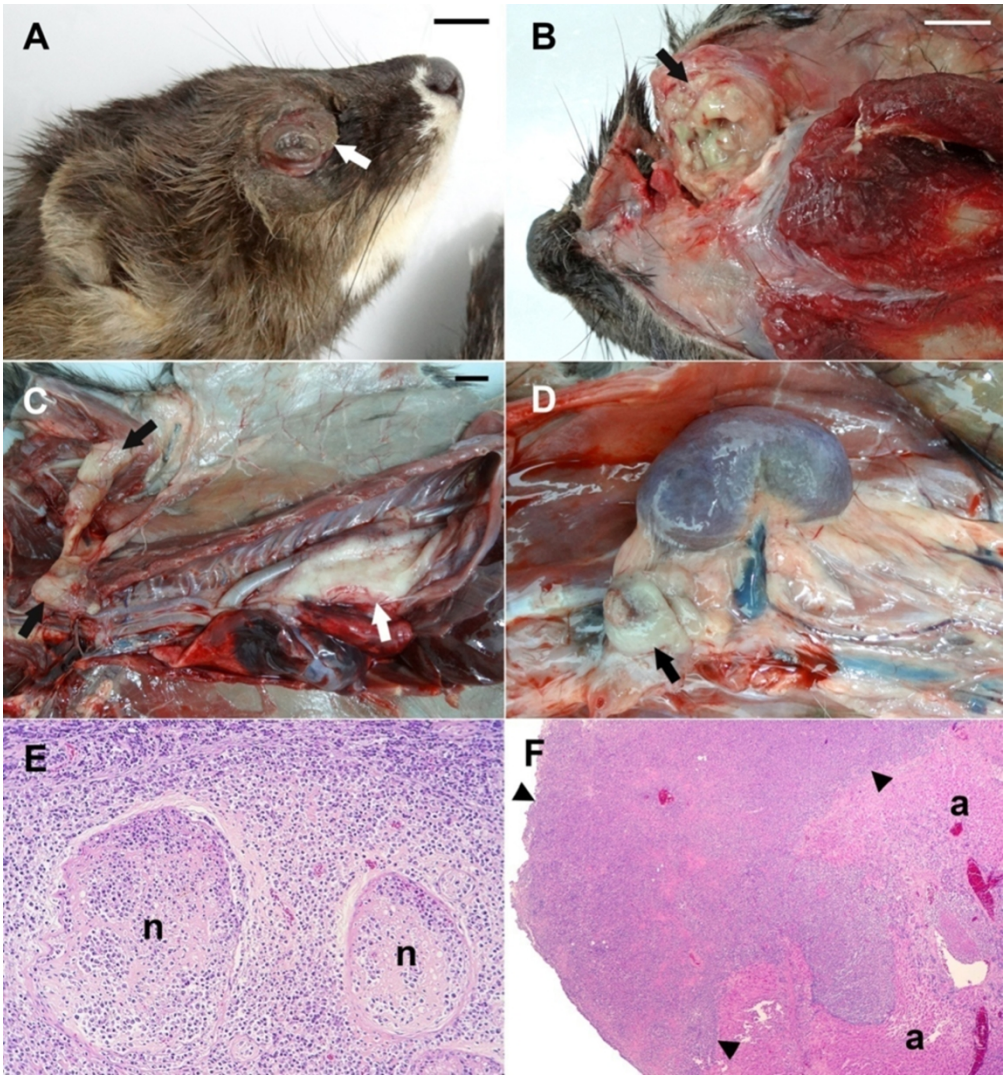

Figure 2. Gross and microscopic findings in European mink (Mustela lutreola) PM-1: (A) Periocular mass (white arrow). Scale bar = 1 centimeter. (B) Retrobulbar mass (right eye, black arrow). Scale bar = 1 centimeter. (C) Perineural mass along the brachial plexus (black arrows) and mediastinal mass (white arrow). Scale bar = 1 centimeter. (D) Mass effacing the left adrenal gland (black arrow). (E) Note diffuse infiltration of neoplastic lymphocytes in the perineural tissues and endoneurium of the brachial plexus mass; n = nerves (hematoxylin and eosin). (F) Adrenal gland (a) is invaded by lymphoma (delimited with arrowheads) (hematoxylin and eosin).

180x192mm (300 x 300 DPI)

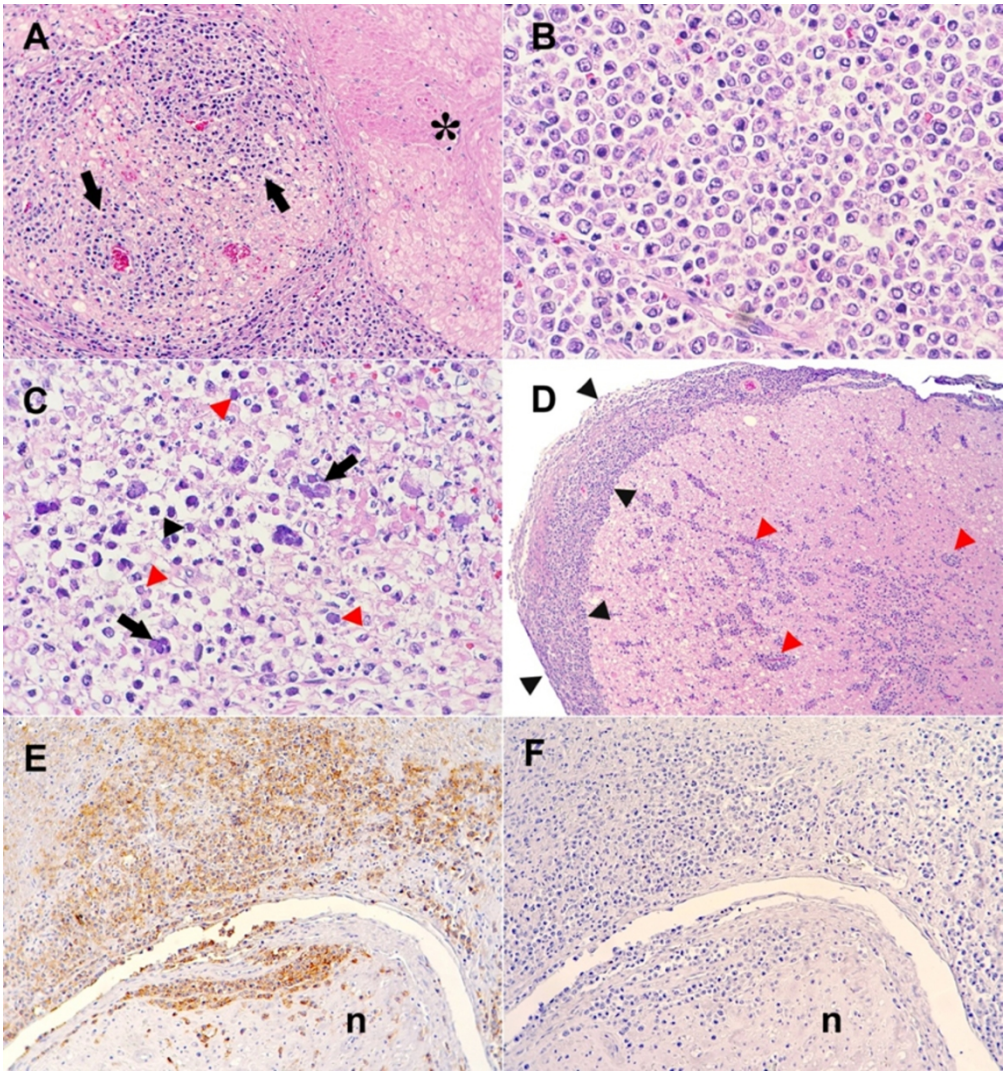

Figure 3. Microscopic and immunohistochemical findings in European mink (Mustela lutreola) PM-1: (A) Higher magnification of endoneural (arrows) and perineural lymphoid infiltrates in the brachial plexus mass. Note necrosis of neural tissue (asterisk). (B) A higher magnification of neoplastic infiltrates demonstrates neoplastic lymphoblasts (hematoxylin and eosin). (C) Note numerous basophilic intranuclear inclusion bodies (red arrowheads) in unidentified cells and syncytia (black arrows) and few eosinophilic intranuclear inclusion bodies surrounded by a clear halo (black arrowhead) in an area of necrosis involving a nerve in the brachial plexus with perineural and neural lymphoma (hematoxylin and eosin). (D) Lymphoma involving the spinal cord, particularly the pachymeninges (delimited with black arrowheads) but also the white and grey matter (red arrowheads) (hematoxylin and eosin). (E) Note positive immunolabeling for CD20 in perineural and endoneural neoplastic lymphocytes in the brachial plexus mass. (F) Neoplastic lymphocytes are not labeled with CD3 antibodies.

180x192mm (300 x 300 DPI)

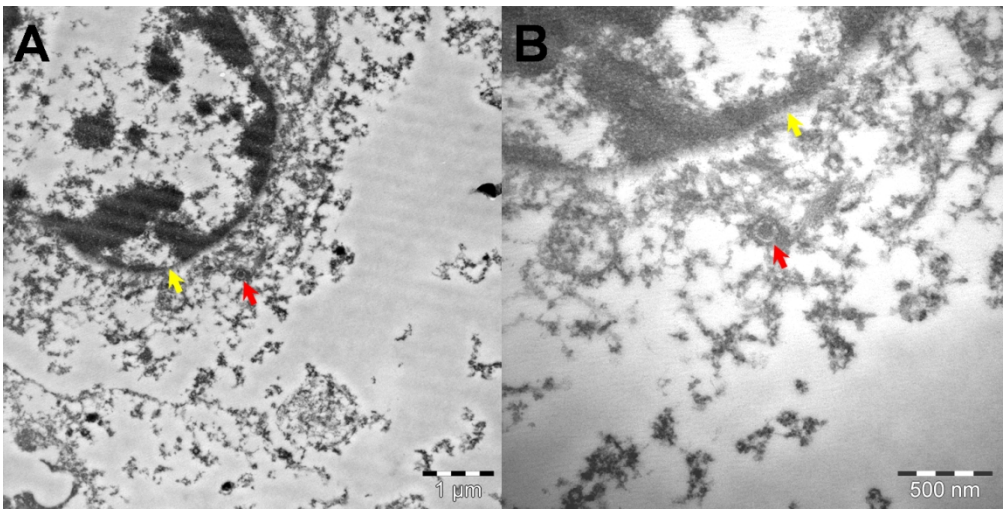

Figure 4. Transmission electron microscopy (TEM) of the perineural lymphoma found in European mink (Mustela lutreola) PM-1: (A) Intracytoplasmic herpesvirus-like particle (red arrow) after nuclear egression but prior to acquiring the secondary envelopment in the cytoplasm (which leads to the well-known enveloped herpesvirus particles seen on mature virions) and nuclear membrane (yellow arrow), (B) Detailed view of the same particle (red arrow) and nuclear membrane (yellow arrow).

125x62mm (300 x 300 DPI)

Table 1. Herpesviruses infections described in the family Mustelidae.

Species	HV name in the article	GenBank access nº.	Lesions attributable to herpesvirus	PCR prevalence	Tissue	Country	Author
European badger (*Meles meles*)	Mustelid herpesvirus 1 (MusHV-1, γ-HV)	AF376034 AY050215 AF275656	Cytopathic effect on badger' pulmonary fibroblasts	Single case	Pulmonary fibroblasts	UK	Banks et al. (2002)
	Mustelid herpesvirus-1 (MusHV-1, γ-HV)	Not provided	Not described	95% (18/19) 100% (10/10)	Blood Blood	UK Ireland	King et al. (2004)
	Mustelid herpesvirus-1 (MusHV-1, γ-HV)	GU799569	Not reported (detected in a road-kill animal)	Single case		Hungary	Dandár et al. (2010)
	Mustelid herpesvirus-1 (MusHV-1, γ-HV)	Not provided	Not described	98.1% (354/361)	Blood	UK	Sin et al. (2014)
	Mustelid gammaherpesvirus 1	AF275657	Not described	Single case	Lung	Not described	Unpublished
	Mustelid alphaherpesvirus 1	MF042164	Not described	Single case	Mediastinal lymph node	France	Unpublished
	Mustelid gammaherpesvirus-1 (MusGHV-1)	Not provided	Not detected	55% (54/98)	Genital swabs	UK	Kent et al. (2018)
Northern sea otter (*Enhydra lutris kenyoni*)	Mustelid herpesvirus-2 (MusHV-2, γ-HV)	GU979535	Presence of ulcers or pale raised plaques on the lingual, gingival, oral, esophageal and labial mucosa: epithelial hyperplasia and hyperkeratosis, often with epithelial cell	46% (13/28)	Skin biopsies	United States	Tseng et al. (2012)

			degeneration and ulceration, and presence of eosinophilic intranuclear inclusion bodies)				
			Apparently healthy animal	34% (21/62)	nasal swabs	United States	
Oriental small-clawed otter (*Aonyx cinerea*)	Oriental small-clawed otter gammaherpesvirus (γ-HV)	FJ797657	Not described	Single case	Not described	Hungary	Unpublished
Captive fisher (*Martes pennanti*)	Fisher herpesvirus (FiHV, γ-HV)	HM579931	Multiple skin ulcers on the muzzle and plantar pads (thickened epidermis with increased numbers of koilocytes, perinuclear vacuolation, nuclear hypertrophy, pale amphophilic intranuclear inclusion bodies, and basophilic pseudoinclusions)	Single case	Skin ulcers	Born in captivity in the Unites States and sent to Canada	Gagnon et al. (2011)
American marten (*Martes americana*)	Marten alphaherpesvirus	KX062131 KX062132 KX062133	Not described	3 cases	Not described	Canada	Dalton et al. (2017)
	Marten betaherpesvirus	KX062129 KX062134 KX062135 KX062136	Not described	4 cases	Not described		

	Marten gammaherpesvirus 1	KX062128	Not described	2 cases	Not described		
	Marten gammaherpesvirus 2	KX062130					
European mink (*Mustela lutreola*)	Mustelid gammaherpesvirus-2	MN082678, MN082679	Basophilic (or eosinophilic, rarely found) inclusion bodies, and syncytia in a multifocal neural and perineural lymphoma.	8.7% (2/23)	Mediastinal B-cell lymphoma and lung	Spain	This work
	Mustelid gammaherpesvirus-3	MN082680	Not detected	8.7% (2/23)	Oral swab, kidney, liver, spleen, bone marrow, brain, spinal cord, sciatic nerve and brachial plexus		

Appendix 1. History of all the European minks from Pont de Suert Captive Breeding Center evaluated in this study. NA= not applicable.

ID	Sex	Weight (grams)	Origin	Birth date	Year of arrival at Pont de Suert	Date of death/euthanasia
LM-1	F	566	Born in Pont de Suert	May 2011	2011	NA
LM-2	F	530	Born in Pont de Suert	May 2016	2016	NA
LM-3	F	618	Born in Pont de Suert	May 2015	2015	NA
LM-4	F	620	Born in Pont de Suert	May 2016	2016	NA
LM-5	F	555	Born in Pont de Suert	May 2014	2014	NA
LM-6	F	566	Born in Pont de Suert	May 2016	2016	NA
LM-7	M	780	Born in Pont de Suert	May 2015	2015	NA
LM-8	M	810	Born in Pont de Suert	May 2015	2015	NA
LM-9/PM-9	M	674	Captured in the wild	May-June 2008†	2012	Oct 2017. Euthanasia
LM-10	M	740	Born in Pont de Suert	May 2013	2013	NA
LM-11	M	912	Captured in the wild	May-June 2015‡	2017	NA
LM-12	M	760	Gipuzkoa captive center	May 2017	2017	NA
LM-13	F	594	Gipuzkoa captive center	June 2016	2017	NA
PM-1	M	960	Born in Pont de Suert	June 2006	Stayed in Captive center in Alava from 2006-2010. Went back to Pont de Suert in 2010	Oct 2015. Euthanasia
PM-2	F	394	Captured in the wild	Unknown	May 2004	Aug 2014. Death
PM-3	M	410	Alava captive center	May 2014	2014	End of 2014. Death
PM-4	F	350	Captured in the wild	Unknown	2004	Oct 2014. Died unexpectedly with no

						premonitory signs
PM-5	F	366	Born in Pont de Suert	May 2007	2007	Oct 2013. Death
PM-6	M	378	Born in Pont de Suert	May 2013	2013	Jul 2013. Death
PM-7	F	310	Born in Pont de Suert	June 2005	2005	Oct 2015. Death
PM-8	F	378	Captured in the wild	Unknown	2004	Jan 2014. Death
PM-10	M	990	Captured in the wild	2012	2015	Oct 2016. Died unexpectedly with no premonitory signs
PM-11	M	980	Born in Pont de Suert	June 2011	2011	Aug 2017. Death during transport

† The animal had to be euthanatized and was subsequently incorporated into the postmortem group with the identification "PM-9". ‡Estimated data.

Appendix 2. Glycoprotein B sequences obtained from the analyzed samples. LM = Live mink. PM = postmortem mink.

ID	Sample number	Samples	HV-Sequence
LM-1	1	Anal swab	0
	2	Conjunctival swab	0
	3	Oral swab	0
	4	Feces	0
	5	Blood	0
LM-2	6	Anal swab	0
	7	Conjunctival swab	0
	8	Oral swab	0
	9	Feces	0
	10	Blood	0
LM-3	11	Anal swab	0
	12	Conjunctival swab	0
	13	Oral swab	0
	14	Feces	0
	15	Blood	0
LM-4	16	Anal swab	0
	17	Conjunctival swab	0
	18	Oral swab	0
	19	Feces	0
	20	Blood	0
LM-5	21	Anal swab	0
	22	Conjunctival swab	0
	23	Oral swab	0
	24	Feces	0
	25	Blood	0
LM-6	26	Anal swab	0
	27	Conjunctival swab	0
	28	Oral swab	0
	29	Feces	0
	30	Blood	0
LM-7	31	Anal swab	0
	32	Conjunctival swab	0
	33	Oral swab	0
	34	Feces	0
	35	Blood	0
LM-8	36	Anal swab	0
	37	Conjunctival swab	0
	38	Oral swab	0
	39	Feces	0
	40	Blood	0

LM-9†	41	Anal swab	0
	42	Conjunctival swab	0
	43	Oral swab	1 (MuGHV-3)
	44	Feces	0
	45	Blood	0
LM-10	46	Anal swab	0
	47	Conjunctival swab	0
	48	Oral swab	0
	49	Feces	0
	50	Blood	0
LM-11	51	Anal swab	0
	52	Conjunctival swab	0
	53	Oral swab	0
	54	Feces	0
	55	Blood	0
LM-12	56	Anal swab	0
	57	Conjunctival swab	0
	58	Oral swab	0
	59	Feces	0
	60	Blood	0
LM-13	61	Anal swab	0
	62	Conjunctival swab	0
	63	Oral swab	0
	64	Feces	0
	65	Blood	0
PM-1	66	Mediastinal lymphoma	1 (MuGHV-2)
PM-2	67	Kidney	0
	68	Lung	0
	69	Liver	0
	70	Peripheral nerve	0
	71	Spleen	0
	72	Brain	0
	73	Lymph node	0
PM-3	74	Kidney	0
	75	Lung	0
	76	Liver	0
	77	Peripheral nerve	0
	78	Spleen	0
	79	Brain	0
	80	Lymph node	0
PM-4	81	Kidney	1 (MuGHV-3)
	82	Lung	0
	83	Liver	1 (MuGHV-3)
	84	Peripheral nerve	0
	85	Spleen	0
	86	Heart	0

	87	Ovary	0
	88	Brain	1 (MuGHV-3)
	89	Lymph node	0
PM-5	90	Kidney	0
	91	Lung	0
	92	Liver	0
	93	Peripheral nerve	0
	94	Spleen	0
	95	Ovary	0
	96	Brain	0
	97	Lymph node	0
PM-6	98	Kidney	0
	99	Lung	0
	100	Liver	0
	101	Peripheral nerve	0
	102	Spleen	0
	103	Brain	0
	104	Lymph node	0
PM-7	105	Kidney	0
	106	Lung	0
	107	Liver	0
	108	Peripheral nerve	0
	109	Spleen	0
	110	Ovary	0
	111	Brain	0
	112	Lymph node	0
PM-8	113	Kidney	0
	114	Lung	1 (MuGHV-2)
	115	Liver	0
	116	Peripheral nerve	0
	117	Spleen	0
	118	Ovary	0
	119	Brain	0
	120	Lymph node	0
PM-9†	121	Kidney	0
	122	Brain	1 (MuGHV-3)
	123	Liver	0
	124	Spleen	1 (MuGHV-3)
	125	Bone marrow	1 (MuGHV-3)
	126	Lymph node	0
	127	Spinal cord	1 (MuGHV-3)
	128	Peripheral nerve-sciatic nerve	1 (MuGHV-3)
	129	Peripheral nerve-brachial plexus	1 (MuGHV-3)
PM-10	130	Spinal cord	0
	131	Lung	0
	132	Peripheral nerve	0

	133	Large intestine	0
	134	Muscle	0
PM-11	135	Liver	0
	136	Brain	0
	137	Cardiac blood	0
	138	Spinal cord	0
	139	Renal lymph node	0
	140	Spleen	0
	141	Kidney	0

† Samples of LM-9/PM-9 correspond to the same European mink; analyzed while alive and after his death.

Appendix 3. Gross and microscopic findings (when available) of herpesvirus-positive animals (PM-1, PM-4, PM-8, PM-9).

ID	Tissue	Gross findings	Microscopic findings	HV
PM-1	Left eye	Corneal opacity	Severe cataracts; mild focal granulomatous conjunctivitis with intralesional vegetal matter; corneal melanosis	NA[†]
	Right eye	Ocular protrusion due a gray-greenish retrobulbar mass (2.5x2x2 cm) Light-tanned periocular mass (eyelid, 0.9x0.4x0.2 cm)	Perineural and neural lymphoma in the retrobulbar mass and the eyelid with invasion of skeletal muscle and skin and intralesional basophilic and rare eosinophilic intranuclear inclusion bodies surrounded by a clear halo and syncytia; severe necrotizing to necrosuppurative neuritis; eyelid thrombosis; foci of acute hemorrhage within the nerves	NA
	Meninges	NSFO[‡]	Lymphoplamacytic infiltrate; rare neoplastic round cells	
	Brain	NSFO	NSFO	NA
	Spinal cord	NSFO	Lymphoma	NA
	Spinal nerves	NSFO	Lymphoma	NA
	Left brachial plexus, left elbow joint nerves, and right sciatic nerve	Light-tanned masses (5.5x1x1 cm mass on left brachial plexus and left elbow joint nerves; size of right sciatic nerve mass was not recorded)	Perineural and neural lymphoma with intralesional basophilic and rare eosinophilic intranuclear inclusion bodies surrounded by a clear halo and syncytia; severe necrotizing to necrosuppurative neuritis; foci of acute hemorrhage	NA
	Lungs	NSFO	NA	NA
	Heart	Concentric hypertrophy of left ventricle	NSFO	NA
	Mediastinum	Light tanned mass (5.5x2.8x2.2 cm) in the caudal mediastinum	Perineural and neural lymphoma with intralesional eosinophilic intranuclear basophilic (or eosinophilic, rarely found) inclusion bodies surrounded by a clear halo and syncytia; severe necrotizing to necrosuppurative neuritis; foci of acute hemorrhage within the nerves	MuGHV-2
	Peripheral skeletal muscle nerves	NSFO	Axonal degeneration	NA
	Unidentified lymph node	NSFO	Severe medullar sinus dilation with high protein lymph and blood resorption products	NA
	Stomach	Without contain	Lymphocytic ganglioneuritis	NA
	Intestines	NSFO	Mild to moderate diffuse lymphoplasmacytic eosinophilic enteritis, with presence of scarce neoplastic lymphoid cells	NA
	Liver	NSFO	Intrahepatocytic vacuoles with eosinophilic matter, and centrilobular distribution; severe hypertrophy and vacuolar degeneration of Ito cells	NA
	Spleen	NSFO	Mild extramedullary hematopoiesis	NA
	Pancreas	Several light tanned nodules, up to 2 mm in diameter	Moderate, multifocal, nodular, acinar hyperplasia	NA
	Prostate	NSFO	Prostatic hyperplasia; glandular ectasia; multifocal, interstitial neutrophilic lymphoplasmacytic prostatitis	NA

	Testicle	NSFO	Focal, acute, necrotizing mixed (neutrophilic and lymphohistocytic) arteritis; mild to moderate, multifocal tubular mineralization	NA
	Kidney	NSFO	Moderate glomerulosclerosis; mild polycystosis; mild multifocal tubular mineralization; and presence of hyaline cast within dilated tubules	NA
	Urinary bladder	NSFO	Leiomyositis; mild, multifocal, acute fibrinohemorrhagic cystitis with intramuscular mucin-rich edema	NA
	Skeletal muscle	NSFO	Non-inflammatory moderate multifocal sarcosporidiosis	NA
	Adipose tissue	Moderate to severe atrophy	Moderate, diffuse adipocyte atrophy	NA
	Adrenal gland	Light tanned mass (1 cm in diameter) involving left adrenal gland	Lymphoma with invasion of the adjacent adipose tissue	NA
PM-4	Brain	NSFO	NA	MuGHV-3
	Peripheral nerve	NSFO	NA	0
	Lung	Congestion	NA	0
	Heart	Hemopericardium	NA	0
	Kidney	NSFO	NA	MuGHV-3
	Liver	Congestion	NA	MuGHV-3
	Spleen	NSFO	NA	0
	Ovary	Left ovarian cyst (2 cm in diameter)	NA	0
	Lymph node	NSFO	NA	0
PM-8	Skin	Large ulceration on the lateral right femoral area	NA	NA
	Brain	NSFO	NA	0
	Peripheral nerve	NSFO	NA	0
	Lung	Congestion	NA	MuGHV-2
	Kidney	NSFO	NA	0
	Liver	Congestion	NA	0
	Spleen	NSFO	NA	0
	Lymph node	NSFO	NA	0
	Ovary	NSFO	NA	0
LM/PM-9	Left eye	Corneal opacity, possible thickening of nictitating membrane	NA	NA
	Brain	NSFO	Mild multifocal spongiosis; mild, arterial (focal) and paquimeningeal mineralization	MuGHV-3
	Spinal cord	NSFO	Mild, multifocal axonal vacuolar degeneration associated with focal gliosis and moderate to marked multifocal meningeal mineralization	MuGHV-3
	Sciatic nerve	NSFO	Multifocal axonal vacuolar degeneration with intra-axonal basophilic inclusion bodies (Lafora bodies)	MuGHV-3

Brachial plexus	NSFO	Autolysis	MuGHV-3
Lymph nodes	Mild generalized lymphadenomegaly	Chronic, severe, diffuse granulomatous lymphadenitis; phagocytosis of silica crystals; intralesional mineralization. Second lymph node: chronic mild to moderate multifocal granulomatous lymphadenitis with medullar sinus dilatation	0
Heart	NSFO	Focal adventitial arterial mineralization	NA
Lungs	Reddish in color, presence of nodular mass (0.5 cm in diameter) in the diaphragmatic left lobe	Well-delimited nodular non-encapsulated adenocarcinoma; mild multifocal subpleural histiocytic and lymphocytic lipid pneumonia	NA
Stomach	Empty stomach	Mild multifocal neutrophilic and lymphoplasmacytic gastritis; multifocal luminal glandular neutrophilic casts	NA
Intestines	NSFO	Mild diffuse lymphoplasmacytic enteritis	NA
Liver	Left liver lobe cystic mass (1.5x1.5 cm)	Biliary cystadenoma; vacuolar degeneration of the Ito cells	0
Spleen	Mild to moderate splenomegaly, 0.5 cm in diameter nodular focal red mass	Nodular hyperplasia; mild diffuse extramedullary hematopoiesis; diffuse blood sequestration	MuGHV-3
Bone marrow	NSFO	Autolysis	MuHHV-3
Kidney	NSFO	Severe membranous glomerulonephritis with tubular dilatation, intratubular hyaline casts, mild multifocal fibrosis and/or interstitial lymphoplasmacytic nephritis and glomerulosclerosis, mild intratubular crystals phagocyted/surrounded by multinucleated giant cells. Tubular polycystosis, one of them associated with atrophy caused by perilesional compression	0
Skeletal muscle	NSFO	Non-inflammatory mild multifocal sarcosporidiosis	NA
Adrenal gland	Pale nodules (< 1 mm in diameter)	Bilateral diffuse nodular hyperplasia of cortical cells	NA
Thyroid gland	NSFO	Moderate nodular or diffuse hypertrophy (hyperplasic goiter)	NA
Parathyroid gland	NSFO	Mild to moderate hypertrophy and cytoplasmic vacuolization of chief cells	NA
Pancreas	NSFO	Mild multifocal nodular ductal hiperplasia; multifocal nodular acinar hyperplasia	NA
Prepuce	Subcutaneous reddish mass (1x0.5x0.3 cm)	Hyperplasia and cystadenomas of preputial glands with focal malignant transformation (to cystadenocarcinoma); purulent adenitis	NA
Testicle	NSFO	Bilateral diffuse atrophy of seminiferous tubules with possible fibrosis/hyalinization of tubular basement membrane; moderate bilateral multifocal mineralization of seminiferous tubules; mild intimal and medial arterial mineralization with mild intimal fibrosis (pampiniform plexus)	NA

† NA= not analyzed; ‡NSFO= no significant findings were observed.